國立臺灣師範大學
地理學系第二十二屆博士論文

Department of Geography

College of Liberal Arts

National Taiwan Normal University

Doctoral Dissertation

台東太麻里溪集水區地景變遷之研究

Analysis of Landscape Changes in the Taimali Watershed of Eastern Taiwan

指導教授：廖學誠

Advisor: Shyue-Cherng Liaw, Ph.D.

研 究 生：葉春國

Chun-Kuo Yeh

中華民國 103 年 6 月

中文摘要

土地覆蓋變遷分析對於提供集水區土地經營、監測及規劃等資訊是極爲重要的。本研究呈現 2005～2011 年間東台灣太麻里集水區大規模地景變遷與其頻繁自然干擾間的關係。爲了解土地覆蓋變遷與自然干擾間之關係，我們採取複合式的地景分析途徑，應用了地景指標、馬可夫鏈模式、改變軌跡及邏輯斯迴歸模式。組成性地景指標分析結果顯示崩塌地面積擴張 7.5 倍（15.52 km^2），而森林面積縮減 10.6%（20.90 km^2）。空間型態地景指標分析結果顯示森林區塊面積變得較小、形狀不規則及空間上破碎；然而，崩塌地區塊面積變得較大及空間上較爲聚集。因此，研究區土地覆蓋變遷主要發生於森林覆蓋的減少和破碎，以及崩塌地數目和面積的增加。在研究期間，地景中最顯著的面積改變是林地轉變爲崩塌地和河道，分別約爲 15.82 km^2 和 6.73 km^2。就轉移機率而言，人爲區塊轉變爲林地和河道的機率爲最大。透過馬可夫鏈的分析，本研究產生了三種各類土地覆蓋比例未來（2017～2035）的預測狀況。三種預測狀況分別被視爲對於下游居民生命及產財具有高、中、低的風險性。

FL、FC 及 VR 三個改變軌跡共占整個集水區全部改變面積的 75.65%，他們被視爲主要的改變趨勢，而且代表太麻里集水區的整體地景（OL）變遷趨勢。改變分析結果顯示地景變遷易發生於畢祿山層地質、鄰近斷層和河道、坡度大於 35°及東向坡的條件下。就模式驗證而言，FC 模式具有最高的 AUC 值。然而，RCI 指標值顯示變遷機率的預測皆能高度符合實際的改變軌跡。因此，本研究得出的四個邏輯斯迴歸模式有助於地景變遷的預測。

關鍵詞：自然干擾、地景指標、馬可夫鏈、改變軌跡、邏輯斯迴歸。

ABSTRACT

Analysis of land cover changes is fundamental for providing information in relation to watershed land management, monitoring, and planning. This study reveals large-scale land cover transformation in relation to frequent natural disturbances within the Taimali watershed in eastern Taiwan during 2005–2011. To understand land cover changes in relation to natural disturbances, a combined landscape analysis approach using landscape metrics, the Markov chain model, change trajectories, and the logistic regression model is used. Results of composition metrics analysis show that areas of landslides within the region had expanded 7.5 times (by 15.52 km^2), but areas of forest had shrunk by 10.6% (20.90 km^2). Spatial configuration metrics analysis indicates that patches of forest are becoming smaller, more irregular, and more spatially fragmented, but that landslide patches are expanding and becoming more spatially aggregated. It is considered that land cover changes in the area have occurred mainly through loss and fragmentation of forest cover, and an increase in the number and area of landslides. During 2005–2011, the most noticeable area changes related to transitions from forest cover to landslides (15.82 km^2) and channels (6.73 km^2). Results show the transition probabilities of human-made patches changing into forest cover and channel corridors are the greatest. Through Markov chain analysis, three future (2017–2035) projections of the proportions of each land cover type are produced. These three predictive statuses are regarded as posing a high, moderate, and low risk, respectively, to life and property downstream.

Three change trajectories, FL, FC, and VR, covering 75.65% of the entire changed area, are considered main changes in trend and represent overall landscape (OL) changes in the Taimali watershed. Results of change analysis indicate that the occurrence of landscape change is subject to the geologic condition of Pilushan Formation, the vicinities of faults and rivers, a gradient greater than 35°, and the eastward slope. As for model validation, the FC model has the highest AUC value. RCI values suggest that the prediction of change probabilities could correspond with the actual change trajectories very well. Therefore, the four logistic regression models are useful tools in the landscape change prediction.

Keywords: natural disturbance; landscape metrics; Markov chain; change trajectory; logistic regression.

CONTENTS

List of Figures

List of Tables

Table Page

1. INTRODUCTION

1.1 Background

Landscape changes are acknowledged as being a part of global environmental change. However, whether such changes are natural or manmade, they are a subject of concern. Landscapes in Taiwan are susceptible to natural disturbances in relation to the country's unique global geographical position. Taiwan is situated on the plate boundary between the Philippine Sea plate and the Eurasian plate, where two arc–trench systems have been interacting since the Miocene (Wu et al. 2006b). Large earthquakes are therefore a major hazard, and their strong motion results in landslides, rock falls, ground displacement, and damages to buildings in the vicinity of the epicenter (Wu et al. 2006b; Wu et al. 2006c). Large earthquakes occur more often in eastern Taiwan in relation to the active arc–continent collision that has a convergence rate of 7–8 cm/year (Wu et al. 2006c).

Taiwan sits on the border between the Tropics and the Subtropics, and as such lies in the way of typhoons as they track their way across the Northwestern Pacific Ocean. Typhoons occur in the summer and autumn every year, bringing extreme rainfall that triggers debris flow, landslides, and floods, and which poses a substantial threat to homes, infrastructure, and life (Chang et al. 2011). Typhoons often strike Taiwan along the eastern coast, and consequently the area is more prone to natural disturbances than other regions.

The Taimali watershed is representative of an area in eastern Taiwan that is susceptible to natural disturbances; and hence is considered to be suitable for an investigation and analysis which will enhance our understanding of land cover change dynamics under the influence of frequent natural disturbances. Studies of land cover changes can contribute to monitoring changes on temporal and spatial scales, and can be used to assess the status of natural resources and predict future changes (Munsi et al. 2010). In addition, land managers can benefit from land cover change mapping, as this provides useful information in relation to watershed land management, monitoring, and planning.

In Taiwan, previous studies of land cover changes under the effects of natural disturbances have focused on central Taiwan, and in particular on the Chenyulan watershed, in relation to the 1999 M_w 7.6 Chi-Chi earthquake and several subsequent large typhoons (Chu et al. 2009; Hong et al. 2010; Lin et al. 2006; Lin et al. 2009; Lin et al. 2010). These studies detected land cover changes using landscape metrics, spatial sampling, simulation, and spatial analysis. However, only limited research has been performed in eastern Taiwan, despite the occurrence of frequent natural disturbances. In addition, few studies have attempted to use the combined landscape analysis approach by applying landscape metrics, Markov chains, change trajectories, and logistic regression to delineate land cover changes, and have only computed the transition matrix, but not predicted future changes (Malaviya et al. 2010; Munsi et al. 2010). To assess land cover changes in the Taimali watershed, this research therefore applies combined landscape analysis and uses three FORMOSAT-2 satellite images, from 2005, 2008, and 2011. The present study provides a new dimension in the understanding of land cover changes within a region experiencing frequent natural disturbances.

1.2 Objectives

This study provides a comprehensive analysis and projection of the dynamics of landscape change induced by the natural disturbances in the Taimali watershed of eastern Taiwan from 2005 to 2011. The landscape change predominantly occurred in the loss and fragmentation of forest cover and the increment in the number and area of landslides. We focus on three land cover types (landslide, forest, and channel), since they provide important information useful to disaster risk assessment at the Taimali watershed. The primary contributions of this paper are to:

(1) detect land cover changes that occurred on a spatio-temporal scale during 2005–2011.

(2) predict the future (2017–2035) possible distribution of land cover according to the use of three different disturbance regimes.

(3) discern the main land cover change trajectories and connect them with environmental variables.

(4) model the probabilities of occurrence of change using logistic regression for four land cover change trajectories.

1.3 Organization

This dissertation is composed of six chapters. The first chapter provides an introduction to the background, objectives, and organization. A review of the literature is presented in detail in Chapter 2 and the review topics contain the theory and application of landscape ecology, Markov chains, land cover change trajectory, and logistic regression. The uses of the materials and methods are demonstrated in Chapter 3. The materials include three landscape images from 2005, 2008, and 2011, three large typhoon events between 2005 and 2011, and historic records of earthquake from 2001 to 2011. The methods employed in the present study contain the landscape metrics analysis, the Markov chains model, the change trajectories analysis, and the logistic regression model. The results are shown in Chapter 4. The topics in this section include: (1) changes in the composition and spatial configuration of land cover; (2) matrices of the area change and transition probability, and predictions of the Markov chains; (3) detection of major change trajectories and their relationship with environmental variables; and (4) modelling the probabilities of occurrence of change trajectories and validation of logistic models. Finally, discussion of the results are presented and some conclusions are drawn in Chapter 5 and 6, respectively.

The flowchart of the study process is illustrated in Fig. 1.1. First, three FORMOSAT-2 satellite images are used to perform image classification. Through accuracy assessment and combination, four landscape elements are detected. Land cover data plus other eight environmental variables are applied to carry out four major research topics using landscape metrics, Markov chains, pixel history, and logistic regression, respectively. All these processes are to achieve the assessment of landscape change in the Taimali watershed of eastern Taiwan.

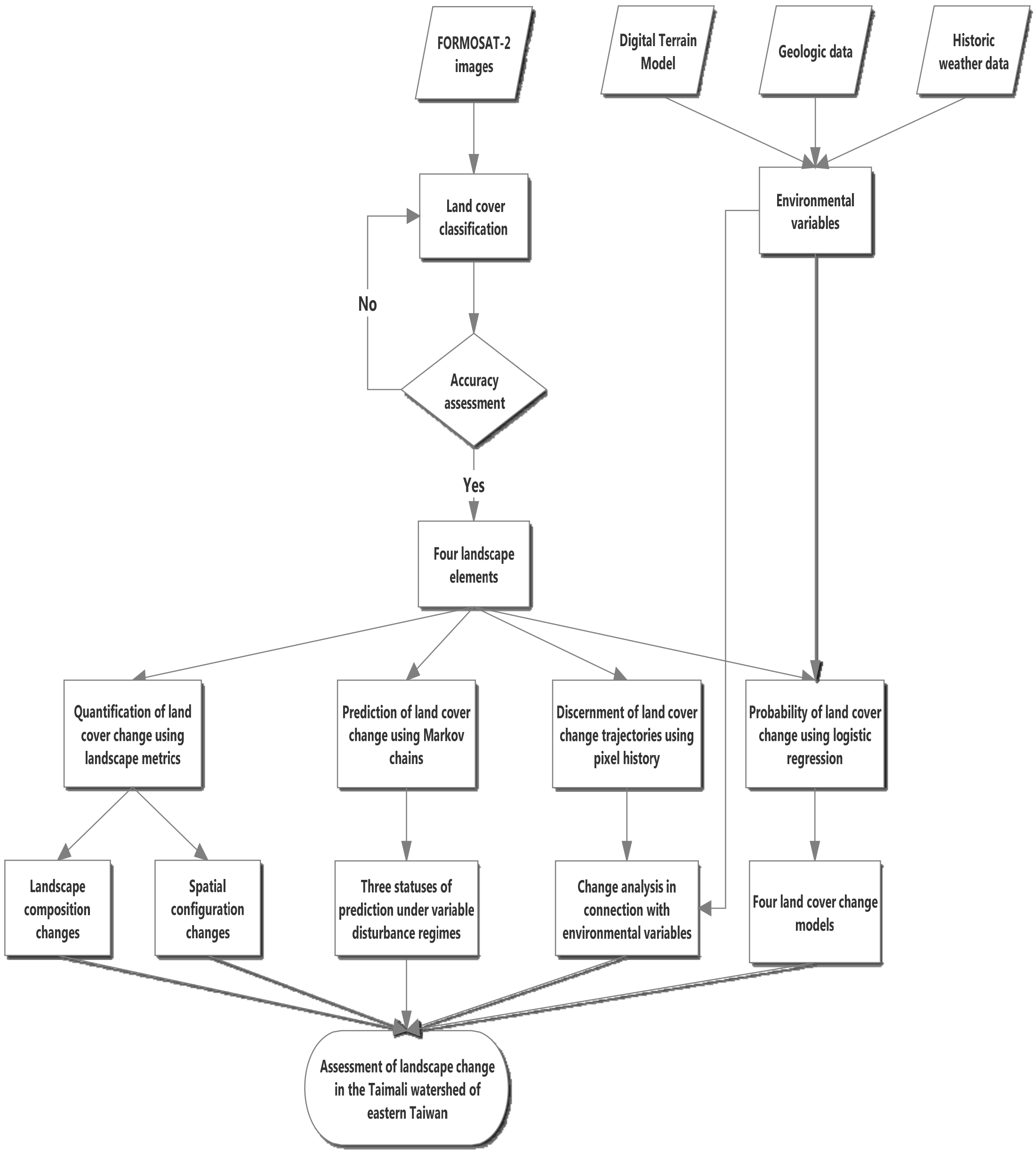

Fig. 1.1 Flowchart of the study process

2. LITERATURE REVIEW

To enhance our understanding about earthquakes and typhoons as a disturbance process on landscape pattern, we take a combined landscape analysis approach that applies landscape metrics, the Markov chain model, change trajectories, and the logistic regression model. These techniques are utilized to assess the effects of typhoons on the characteristics of land cover change, to predict possible trends for the future, and to map probabilities of change for the main change trajectories.

2.1 Landscape ecology and the applications of landscape metrics

Landscape ecology is simply the ecology of landscapes and a landscape is described as a kilometer-wide mosaic where the mix of local ecosystems or land uses is repeated in a similar form (Forman 1995). Nevertheless, when the emphasis is placed on spatial heterogeneity, the concept of landscape as a spatial mosaic can be at various spatial scales from the beetle's lifeworld within a few square meters to nitrogen dynamics in a watershed (Turner et al. 2001). A landscape mosaic is composed of three types of landscape elements that are relatively homogeneous units recognized at the landscape scale and refer to patches, corridors, and a background matrix (Forman 1995). The subjects of study in landscape ecology are the three landscape characteristics, inclusive of structure (form), function, and change (Forman 1995; Zonneveld 1990). Structure refers to the numbers, sizes, shapes, kinds, and spatial pattern or arrangement of landscape elements; function refers to the flows of energy, materials, and organisms through the structure; and change refers to the dynamics or alteration in the structure and function over time (Dramstad et al. 1996; Turner 1989). Therefore, developing quantitative methods are necessary to describe the landscape structure, compare different landscapes, identify significant changes over time, and relate landscape patterns to ecological function (Turner 1989).

Landscape metrics, derived from information theory, describe and quantify landscape patterns that are linked to ecological processes and can predict them on a broad scale (Turner, 1989; Turner et al. 2001). Many studies have demonstrated the importance of the application of landscape metrics in quantifying landscape patterns, their changes over time, and their effects on ecological processes (Antwi et al. 2008; Frondoni et al. 2011; Kintz et al. 2006; Paudel and Yuan, 2012). These metrics of landscape status can be applied to correlate with specific aspects of ecosystem function; therefore changes in metrics are indicators of changes in the ecological condition of the landscape (O'Neill et al. 1997). Besides, on account of the interplay between spatial patterns and ecological processes, landscape metrics can inform environmental planners about landscape functions that are usually difficult or impossible to measure directly (Botequilha Leitão et al. 2006). Olsen et al. (2007) further indicated that the use of landscape metrics is important in building an effective environmental monitoring system.

2.2 Applications of Markov chains

A Markov chain is a stochastic process, and represents a system of elements undergoing transitions from one state to another over time. It can be parameterized by empirically estimating transition probabilities between discrete states in the observed system (Balzter, 2000). Tattoni et al. (2011) indicated that Markov chains were useful mathematical tools for modeling a process with a finite number of states and known probabilities of moving from each state to the others. Reddy et al. (2008) also suggested that the Markov chain analysis was a convenient tool for modeling land use change because it was difficult to describe changes and processes in the landscape.

Apart from quantifying land use changes, the Markov model procedure can reveal obscure data trends (Muller and Middleton 1994). Therefore, the Markov chain analysis can describe land cover changes from one time point to another, and it further employs this information as the basis to predict future changes. Performing the Markov chain analysis first requires the computation of the transition probabilities that are reported in a matrix showing the rates of transition between states (Tattoni et al. 2011).

Markov chains have been widely applied to model changes in land use and land cover from nature-dominated to human-dominated landscapes on a variety of spatial scales. With respect to natural landscapes, research has mostly been related to deforestation, vegetation recovery, forest succession, etc. Through calculating transition probability, Reddy et al. (2009) found that extensive deforestation of Nawarangpur in India resulted from forest converting into agriculture land. In the study of landslide areas in central Taiwan, the Markov chain model was applied for vegetation recovery assessment and simulating future land cover changes was based on the transitive probability matrix (Chuang et al. 2011). In addition, from the examples of Erzgebirge in Germany, the results showed that Markov chain models were an efficient tool to organize the existing knowledge of forest succession into a system of quantitative predictions (Benabdellah et al. 2003). In relation to human-modified landscapes, research has mostly focused on urban expansion. In a case study of Beijing which is a mega city of China, Wu et al. (2006a) found that urban that growth engulfed the surrounding agriculture lands in suburbs and they projected land use changes for the next 20 years with the application of Markov chains and regression analyses. The same examples that croplands were replaced with urban development could be found in the studies of Muller and Middleton (1994) and Weng (2002).

The disturbance regime of a landscape refers to the spatio-temporal dynamics of disturbances over a prolonged period of time, using characteristics such as spatial distribution, frequency, size, and intensity. It remains a current topic of active research that aims to improve our quantitative understanding and ability to predict the effects of changing disturbance regimes on landscape patterns (Turner et al. 2001). In the Taimali watershed, each typhoon and earthquake event causes a varying degree of change to the landscape, due to the differing size, intensity, and frequency of each event. This research uses transition probabilities calculated from different time periods as a proxy for variable disturbance regimes, with the aim of predicting future land cover changes under varying statuses of disturbance regimes.

2.3 Land cover change trajectory

From a methodological point of view, there are four different ways to quantify land cover changes, including: (1) simple measures of change, like the proportion of change, (2) annual rates of change, (3) changes in the spatial arrangement or structure of land cover, and (4) spatially-explicit representations of change at the pixel level using the concept of pixel histories (Mena 2008). The fourth approach described above is namely the change trajectory that tracks pixel histories across the time series (Rindfuss et al. 2004). Land cover change trajectories refer to a succession of land cover types for a given sampling unit in the raster images of time series over more than two observation years (Mertens and Lambin 2000; Zhou et al. 2008a; Zhou et al. 2008b). Land cover change can be combined to create a high diversity of change trajectories that are determined by the local conditions, regional contexts, government policies, and external influences (Mertens and Lambin 2000; Verburg et al. 2010). By coupling the change history with a specific region, trajectories not only allow the illustration of change patterns in temporal dimension, but also consider their continuity and direction (Ruiz and Domon 2009).

The notion of trajectory, targeting at identifying the paths by which landscapes change over time, has recently drawn a lot of attention in studies of landscape change analysis (Ruiz and Domon 2009). By means of classification of land cover change trajectories, researchers could find the main driving forces of the landscape changes, which were dominated by natural forces or human activities. A small case study in the Northern Intensive Study Area of Northern Ecuadorian Amazon showed that agricultural trajectories which included pasture and large and small scale agriculture were the dominant change trajectories causing the loss of forest (Mena 2008). Zhou et al. (2008a and 2008b) demonstrated a research on land cover change trajectories in the fragile ecosystem of China's arid environment and the results indicated that natural forces such as floods were dominant in environmental change; however, human impact, such as cultivation and dam/reservoir construction, has increased dramatically in recent years. In a study of highly dynamic landscape in southern Chile, Carmona and Nahuelhual (2012) found that the trajectories of deforestation and forest degradation, which converted from old growth forest to scrubland and secondary forest, respectively, were the two most important groups of change trajectories.

Obtaining comprehensive knowledge of the dynamics of land cover changes could be beneficial to reconstruct past land cover changes, discern their main driving forces, predict future changes, and thus help develop sustainable management practices pointing at preserving fundamental landscape functions (Domon and Bouchard 2007; Hietel et al. 2004). This study tries to show that the analysis of land cover change trajectories can be spatially explicit in response to the dynamics of natural disturbances. In addition, for a case study reconstituting the landscape of Godmanchester (Quebec, Canada), Domon and Bouchard (2007) emphasized that the research on landscape dynamics must not only allow the recording of the transformations and their consequences, but also attempt to explain them by identifying the relationships between the biophysical, anthropic and technological factors. Since the study area is a mountainous watershed and the area of human activity is less than 1.84% of the entire watershed, this paper also attempts to reveal the relationships between change trajectories and physical environmental conditions.

2.4 Logistic regression

One of our research objectives is to develop a spatially-explicit model for predicting the probability of land cover change in the Taimali watershed based on geological, meteorological, topographical, and distance-related factors selected according to their importance to the landscape change and data availability. Land cover trajectories can be divided into two categories: stable versus dynamic trajectories (Mena 2008). Stable trajectories are characterized by pixel histories that are unchanging across the time-series while dynamic ones are described by pixel histories with varied classes over time. For each pixel's trajectory type, it is either stable or dynamic; therefore the dependent variable is a binary variable.

Due to the characteristics of the dependent variable, logistic regression was found to be the most suitable method for analyzing the probability of land cover change and hence employed in the present study. Logistic regression is a method for estimating the probability of occurrence of an event from dichotomous data, using a set of variables which may be continuous, discrete, or a combination of both (Bui et al. 2011). The logistic regression has two main advantages. One is that independent variables do not necessarily have normal distributions; the other is that the predicted values are expressed as probabilities lying in the range between 0 and 1 giving the risk of event occurrence in an area (Kleinbaum and Klein 2010).

Many researches simultaneously applied the concept of pixel history and the method of logistic regression analysis to estimate the probability of land cover change for every pixel while they often focused on landslide hazard assessment. Taking a case study in Central Taiwan for instance, the logistic regression results revealed that the frequency of landslide occurrence played an important role in assessing landslide hazards (Lin et al. 2010). Besides, analyzing historical and recent landslides in the northeastern Ohio, U.S.A., Nandi and Shakoor (2009) suggested that the multivariate logistic regression model, compared with bivariate statistical analysis, was the better model in predicting landslide susceptibility. In fact, relatively few studies were found to assess the probability of change on every pixel for land cover change trajectories (Braimoh and Vlek 2005; Mena 2008). An example from Northern Ecuadorian Amazon (NEA), Mena (2008) mapped the probability of landscape transitions using logistic regression analysis. The results demonstrated that the landscape of the NEA was more dynamic at its core rather than in the periphery. Therefore, binary logistic regression was utilized to model the probability of change, i.e., risk of occurrence of change trajectories, for a given set of independent variables.

3. MATERIALS AND METHODS

3.1 Study area and disturbance events

The study area used in this research is the Taimali watershed, a region susceptible to earthquake and typhoon occurrence in eastern Taiwan (Fig. 3.1). Located in Taitung County, it is a typical mountainous watershed. The Taimali stream moves in a direction from west to east before finally flowing into the Pacific Ocean. The watershed rises to a height of 3000 m, with an average elevation of 935.4 m, (almost 35% of the entire watershed area is over 1000 m). It measures about 27 km in length, is west–east oriented, and stretches from the Taimali stream estuary on the eastern boundary to Mount Dawu on the western border. This watershed also has a total area of 211.5 km^2 and an average gradient of 57.6%.

Based on historic records from 2001–2011 provided by the Central Weather Bureau (CWB) of Taiwan, three earthquakes with Moment magnitudes (M_w) greater than 6 (and seismic intensities estimated as 5) have occurred in the vicinity of the Taimali watershed (Table 3.1). The Chengkung earthquake occurred in eastern Taiwan in 2003, causing landslides, rock falls, and construction damage in the epicentral area (Wu et al. 2006c). The 2006 Taitung earthquake produced significant ground displacement, and a large numbers of aftershocks occurred throughout the following month (Wu et al. 2006b). The 2010 Jiashian earthquake in SW Taiwan caused moderate damage, but no surface rupture was observed, implying a deep source, which is a relatively rare occurrence in western Taiwan (Huang et al. 2013). However, although no deaths were reported, 96 people were injured, and two high speed trains were disrupted at the time of quake due to ground shaking (Rau et al. 2012).

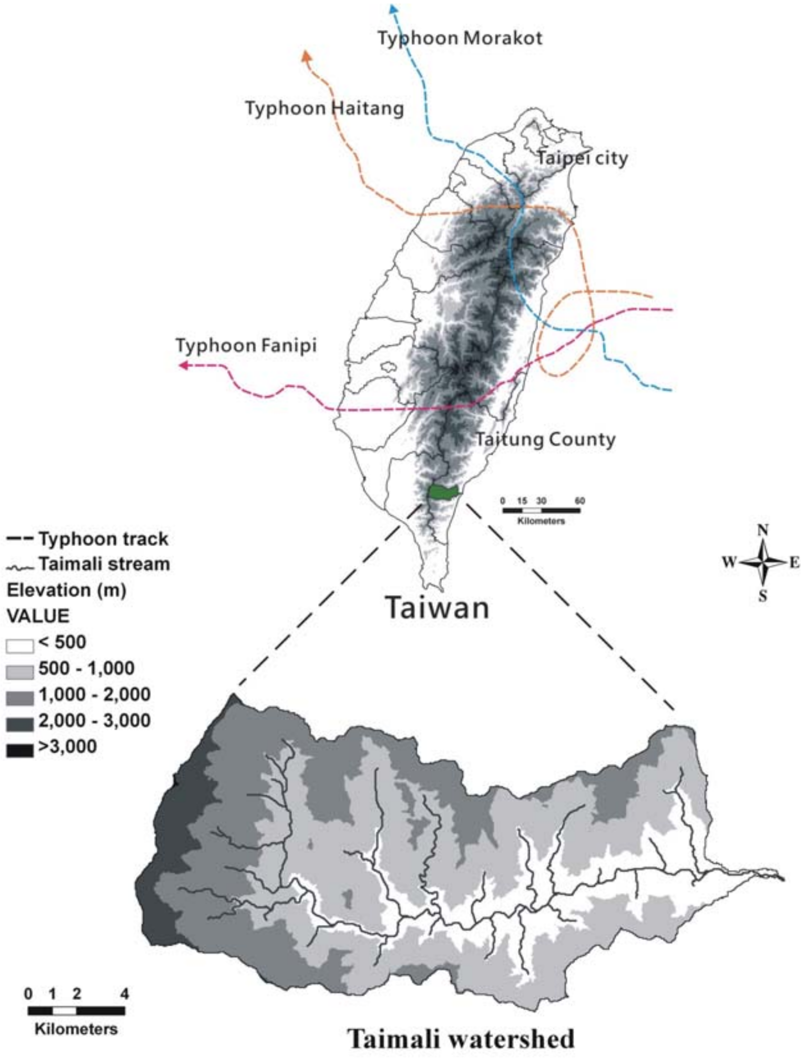

Fig. 3.1 Location of the study area with typhoon tracks

Table 3.1 Earthquake occurrence in the vicinity of the study area

Name	Date	GMT+08:00 (Taiwan)	Latitude (°N)	Longitude (°E)	Depth (km)	M_w	Largest intensity at Taimali
Chengkung earthquake	10/12/2003	12:38:13.5	23.07	121.40	17.7	6.8	5
Taitung earthquake	01/04/2006	18:02:19.5	22.88	121.08	7.2	6.1	5
Jiashian earthquake	04/03/2010	08:18:52.1	22.97	120.71	22.6	6.3	5

Moment magnitude (M_w) based on Wu et al. (2006b), Wu et al. (2006c), and Huang et al. (2013); all other information obtained from the CWB.

Typhoons usually strike Taiwan along the eastern coast, and as the mouth of the Taimali watershed faces east and is adjacent to the Pacific Ocean the area is susceptible to typhoons. Information related to typhoon occurrence in eastern Taiwan was obtained from the typhoon database provided by the CWB of Taiwan. During 2005–2011, a total of 23 typhoons hit Taiwan, and of these three fierce typhoons struck the Taimali watershed (Fig. 3.1). Firstly, the center of Typhoon Haitang swept across northern Taiwan from the east towards the west on July 18, 2005, with a maximum wind speed of 55.0 m/s and a radius of 280 km (CWB 2005). This typhoon caused heavy rainfall and subsequent significant flooding, which destroyed infrastructure and houses in the Taimali watershed. Typhoon Morakot then occurred on August 7–8, 2009; its center moved from east to northwest with a maximum wind speed of 40.0 m/s and a radius of 250 km (CWB 2009). Typhoon Morakot brought record-breaking torrential rainfall that triggered serious flooding, debris flow, and landslides in eastern, central, and southern parts of Taiwan; causing a tremendous amount of damage to property and infrastructure in the Taimali watershed. On September 19–20, 2010, the center of Typhoon Fanapi then passed through central Taiwan from east to west, with a maximum wind speed of 45.0 m/s and a radius of 200 km (CWB 2010). This typhoon produced heavy rainfall in the eastern and central regions of Taiwan, and the flooding that occurred in the Taimali stream flushed away several buildings and approximately 120 m of rail track.

The typhoons described here caused both the destruction and creation of land cover, thereby resulting in land cover change.

3.2 Landscape image and classification

To obtain land cover data, three FORMOSAT-2 satellite images from 2005, 2008, and 2011, with spatial resolutions of 8 m and minimal cloud cover, were acquired from the Spatial Information Research Center (SIRC) of the National Taiwan University. At our request, three images underwent preprocessing of geo-registration, rectification, and projection into the Transverse Mercator coordinating system by the SIRC. ERDAS IMAGINE version 9.2 software (Leica Geosystems, Inc.) was employed to perform the image classification. Field investigation and land cover maps of the Taimali watershed produced by previous studies were used as reference information to successfully accomplish the land cover classification and the subsequent accuracy assessment. Six types of land cover were identified (including landslide, forest, farmland, buildup, channel sand, and water) using the supervised classification method and the parametric rule of maximum likelihood. In the present study, "forest" is defined as a mixture of grassland and woodland. Each land cover type was recognized using several training samples, and the number of training samples was based on the size and degree of the spatial dispersion of a specific class. Table 3.2 demonstrates the accuracy assessment of land cover classification evaluated from 256 randomly generated reference points obtained from using stratified random sampling (Xiao and Ji 2007). All the overall accuracies and Kappa coefficients are shown to be greater than 83.90% and 0.80, respectively. Since "farmland" and "buildup" were seen to cover a smaller area, both of these land cover types were combined and then categorized as "human-made patches" to simplify the information. The land cover types, "water" and "channel sand" were also combined as "channel corridors" for the same purpose. Therefore, four landscape elements: landslide patches, forest matrix, human-made patches, and channel corridors were used for the analysis of landscape changes. In addition, to explicitly detect changes in channel width, channel corridors were digitized using ArcGIS version 9.3.1 in three satellite images. To retain the connectivity of channel corridors, all classified images originally had a pixel size of 8 m, but were converted to a pixel size of 4 m to facilitate further analysis. The resulting three sets of land cover data were then used to calculate landscape metrics in 2005, 2008, and 2011, respectively, along with their transition probabilities.

Table 3.2 The results of accuracy assessment (%)

	2005	2008	2011
Landslide	77.08/92.50	82.22/90.24	68.97/80.00
Forest	98.21/100.00	92.98/98.15	96.45/95.32
Farmland	92.86/95.12	83.72/90.00	76.47/92.86
Buildup	93.94/77.50	89.47/42.50	100.00/54.55
Channel sand	81.58/77.50	68.63/85.37	74.07/80.00
Water	97.44/95.00	90.24/92.50	87.50/70.00
Overall accuracy	90.23	83.98	89.45
Kappa coefficient	0.882	0.807	0.801

77.08/92.50 indicates Producer’s accuracy/User’s accuracy.

3.3 Landscape metrics

A large number of landscape metrics or indices have been developed and used to characterize a wide variety of spatial patterns (Gustafson 1998; O’ Neill et al. 1997). Spatial patterns have an influence on a wide variety of ecological processes, which then in turn influence the spatial patterns (Botequilha Leitão et al. 2006). Landscape metrics are able to measure the composition and spatial configuration of landscape elements; in this context, composition refers to features associated with the variety and abundance of patch types within the landscape, without reference to spatial attributes, and spatial configuration refers to the spatial character and arrangement, position, or orientation of patches within the class or landscape (McGarigal et al. 2012). In our research, we utilized nine class-level metrics calculated by FRAGSTATS version 4.0, including Class Area (CA), Percentage of Landscape (PLAND), Mean Patch Area (AREA_MN), Edge Density (ED), Mean Shape Index (SHAPE_MN), Mean Patch Fractal Dimension (FRAC_MN), Number of Patches (NP), Mean Euclidean Nearest-Neighbor Distance (ENN_MN), and Aggregation Index (AI) (Table 3.3). The first two metrics belong to composition metrics and the others belong to spatial configuration metrics. We calculated class-level metrics because each land cover type provides different information in relation to watershed management at Taimali. These metrics were selected because they were able to assess the variation in aspects of the landscape's characteristics. They measure the aspects of the patches, which includes proportional abundance, area, edge, shape complexity, subdivision, isolation, and aggregation. Subdivision refers to the degree to which a patch type is broken up into separate patches. Isolation deals with the degree to which patches are spatially isolated from each other, and aggregation refers to the tendency of patch types to be spatially aggregated (and it is an umbrella term used to describe several related concepts, including subdivision and isolation) (McGarigal et al. 2012).

Table 3.3 Class-level landscape metrics used in this study

Metrics	Abbreviation	Unit	Description
Class Area	CA	ha	Measuring how much of the landscape is comprised of a particular patch type
Percentage of Landscape	PLAND	%	Quantifying the proportional abundance of each patch type in the landscape
Mean Patch Size	AREA_MN	ha	Measuring landscape configuration by the average condition of patch size
Edge Density	ED	m/ha	Standardizing edge to a per unit area basis that facilitates comparisons among landscapes of varying size
Mean Shape Index	SHAPE_MN	none	Measuring the complexity of patch shape compared to a standard shape (square) of the same size
Mean Patch Fractal Dimension	FRAC_MN	none	Characterizing patch shapes via the fractal dimension of the object
Number of Patches	NP	none	Measuring the extent of subdivision or fragmentation of the patch type
Mean Euclidean Nearest-Neighbor Distance	ENN_MN	m	Measuring patch isolation by using simple Euclidean geometry
Aggregation Index	AI	%	Measuring aggregation based on the ratio of the observed number of like adjacencies to the maximum possible number of like adjacencies

The computation and description of metrics are based on FRAGSTATS 4.0 (McGarigal et al. 2012).

3.4 Markov chains

A Markov chain, defined as a stochastic process, shows that the value of a process at time t, X_t, depends only on its value at time $t-1$, X_{t-1}, and not on the sequence of values $X_{t-2}, X_{t-3}, \ldots, X_0$ that the process passed through before arriving at X_{t-1} (Weng 2002). It can be expressed as follows (Wu et al. 2006a):

$$P\{X_t = j | X_{t-1} = i,\ X_{t-2} = i_{t-2}, \ldots, X_0 = i_0\} \tag{3.1}$$
$$= P\{X_t = j | X_{t-1} = i\}$$

The conditional probabilities $P\{X_t = j | X_s = i\} = p_{ij}(s,t)$ are called transition probabilities of order $r = t - s$ from state i to state j for all indices $0 \leq s < t$, with $1 \leq i, j \leq$ k, and are denoted as the transition probability matrix *P* (Balzter 2000; Logofet and Lesnaya 2000). For *K* states, the first-order Markov transition matrix *P* takes the form:

$$P = \begin{bmatrix} p_{11} & p_{12} & \cdots & p_{1\mathrm{k}} \\ p_{21} & p_{22} & \cdots & p_{2\mathrm{k}} \\ \cdots & \cdots & \cdots & \cdots \\ p_{\mathrm{k}1} & p_{\mathrm{k}2} & \cdots & p_{\mathrm{kk}} \end{bmatrix} \tag{3.2}$$

The future distribution of states X_t can be calculated by multiplying the initial distribution of states X_{t-1} with the state transition probability matrix *P* having elements p_{ij} that represent transition probabilities from state i to state j, and can be expressed as (Baasch et al. 2010):

$$X_t = P \times X_{t-1} \tag{3.3}$$

In practical application of Markov chain analysis, researchers are initially required to establish a transition probability matrix of land cover changes from one time point to another. The matrix shows the character of change at each land cover type, and can then serve as a basis for projecting the proportion of land cover at any considered future time period. In the present study, future projections (2017–2035) of land cover changes under different disturbance regimes were performed using the Markov chain.

3.5 Method of trajectory calculation

Our objective is to acquire a categorical map that demonstrated the pixel history, namely land cover trajectories, at the pixel level. The categorical map can be called the trajectory layer. Each land cover class is described as a code in the land cover raster layer. In the present study, codes in the land cover raster layer from 1 to 4 represent the landslide patch, forest matrix, human-made patch, and channel corridor, respectively. To make the codes in the land cover layers of year 2005, 2008, and 2011 discriminative to each other, the three land cover layers are multiplied by 100, 10, and 1, respectively, and then they are summed to obtain a trajectory layer.

The trajectory layer shows a sequence of codes for every pixel, which can be called trajectory codes. When there are less than ten classes of land cover, the trajectory codes can be calculated by the following formula (Mena 2008; Wang et al. 2012; Wang et al. 2013):

$$\mathrm{TC_{ij}} = (\mathrm{C_{t1}})_{\mathrm{ij}} \times 10^{\mathrm{n}-1} + (\mathrm{C_{t2}})_{\mathrm{ij}} \times 10^{\mathrm{n}-2} + (\mathrm{C_{tn}})_{\mathrm{ij}} \times 10^{\mathrm{n}-\mathrm{n}} \quad (3.4)$$

where $\mathrm{TC_{ij}}$ is the trajectory code of pixel at row i and column j in the trajectory layer; n is the quantity of the time points; $(\mathrm{C_{t1}})_{\mathrm{ij}}$, $(\mathrm{C_{t2}})_{\mathrm{ij}}$, and $(\mathrm{C_{tn}})_{\mathrm{ij}}$ are the codes in land cover layers of different time points at the given pixel, and they have to be ranked by time points in ascending order.

3.6 Environmental variables in relation to change trajectories

To realize the relationship between the changed area and the environmental variables, we first convert the map of the main land cover change trajectories into a binary map composed of the changed area and unchanged area. Second, we need to prepare the distribution maps of related environmental variables, and then overlay the binary map with them to calculate the percentage and intensity of land cover change in each subregion of the distribution map of environmental variables.

3.6.1 Environmental variables of the study area

The environmental variables are listed in Table 3.4 and are described respectively as follows:

(1) Lithology

Lithology is considered an underlying driving factor in the research exploring the relationship between landslides and environmental factors (Bai et al. 2010; Lin et al. 2010; Bui et al. 2011). Since landslide occurrences are the most significant event of land cover change in the study area, the lithology variable is included in the analysis. Geological formations of the study area are composed of three strata, inclusive of Pilushan Formation, Lushan Formation, and Tananao Schist (Fig. 3.2). Lithological characteristics are identified according to Ho (1986). Pilushan Formation is an Eocene system and mainly consists of slate and phyllite. Lushan Formation, a Miocene system, primarily contains charcoal graywacke interbeded with black-charcoal argillite, slate, and phyllite. Tananao Schist, a Pre-Tertiary metamorphic complex, is made up of various schists and marble, both of which are metamorphosed from sedimentary and volcanic rocks.

(2) Distance to faults

There are two faults in the study area and their spatial distribution is similar to the letter Y shape (Fig. 3.3). One passes across the central part of Taimali watershed in a north-south direction and the other is elongated in a north-east to south-west direction at the northern part of Taimali watershed. The distance to faults is calculated by measuring the straight-line distance to faults with ArcGIS Spatial Analyst tools and is classified into five classes, including 0-2000 m, 2000-4000 m, 4000-6000 m, 6000-8000 m, and ＞8000 m (Fig. 3.3).

(3) Rainfall

Since there is no rainfall station in the study area, kriging interpolation is applied to estimate the average annual rainfall of the study area. Average annual rainfall map is produced by utilizing the ordinary Kriging method with the spherical semivariogram model to interpolate a surface from the neighboring twelve rainfall stations. Average annual rainfall is divided into four classes, inclusive of 2000-3000 mm, 3000-4000 mm, 4000-5000 mm, and 5000-6000 mm (Fig. 3.4).

(4) Distance to rivers

Distance to rivers is calculated by measuring the straight-line distance to Taimali stream in 2005 with ArcGIS Spatial Analyst tools and is classified into five classes, including 0-300 m, 300-600 m, 600-900 m, 900-1200 m, and ＞1200 m (Fig. 3.5).

(5) Elevation

Elevation data are taken from a digital terrain model (DTM) provided by the Aerial Survey Office, Forestry Bureau, Council of Agriculture, R.O.C. The resolution of DTM is 40 × 40 m. Elevation is categorized into six classes, inclusive of 0-500 m, 500-1000 m, 1000-1500 m, 1500-2000 m, 2000-2500 m, and ＞2500 m (Fig. 3.6).

(6) Slope

The slope gradient is extracted from the DTM and then divided into six slope gradient categories, including 0°-5°, 5°-15°, 15°-25°, 25°-35°, 35°-45°, and ＞45° (Fig. 3.7).

(7) Aspect

The slope aspect is also obtained from the DTM and the resulting aspect image is classified and labeled with 9 identifiers based on Miliaresis (2008) (Fig. 3.8). In the distribution map of aspect, azimuth N stands for aspects in the range 337.5° to 22.5°, NE for 22.5° to 67.5°, E for 67.5° to 112.5°, SE for 112.5° to 157.5°, S for 157.5° to 202.5°, SW for 202.5 ° to 247.5°, W for 247.5° to 292.5°, NW for 292.5° to 337.5°, and F for flat terrain that is an undefined aspect.

(8) Curvature

Curvature is mathematically defined as the change in slope angle along a very small arc of the curve, and can be expressed as the inverse of the radius of a circle which is tangent over a small arc of the curve (Ohlmacher 2007). A positive curvature indicates that the surface is a convex landform at that cell (e.g., hill and ridge), a negative curvature indicates that the surface is concave landform at that cell (e.g., depression and valley), and a curvature of zero indicates that the surface is flat (Florinsky 2012). The distribution map of the curvature is presented in Fig 3.9.

Table 3.4 Independent variables used in the logistic regression model

Independent variables	Type	Unit	Range	Source
Lithology	Categorical	–	–	Central geological survey, MOEA, R.O.C.
Distance to faults	Continuous	Meters	0–14295.73	Central geological survey, MOEA, R.O.C.
Rainfall	Continuous	Millimeters	2457.08–5641.97	Water Resources Agency, MOEA, R.O.C.
Distance to rivers	Continuous	Meters	0–2863.56	Digital Terrain Model
Elevation	Continuous	Meters	3–3090	Digital Terrain Model
Slope	Continuous	Degrees	0–82.60	Digital Terrain Model
Aspect	Categorical	Degrees	0-360	Digital Terrain Model
Curvature	Continuous	1/hectometer	-105.94–56.75	Digital Terrain Model

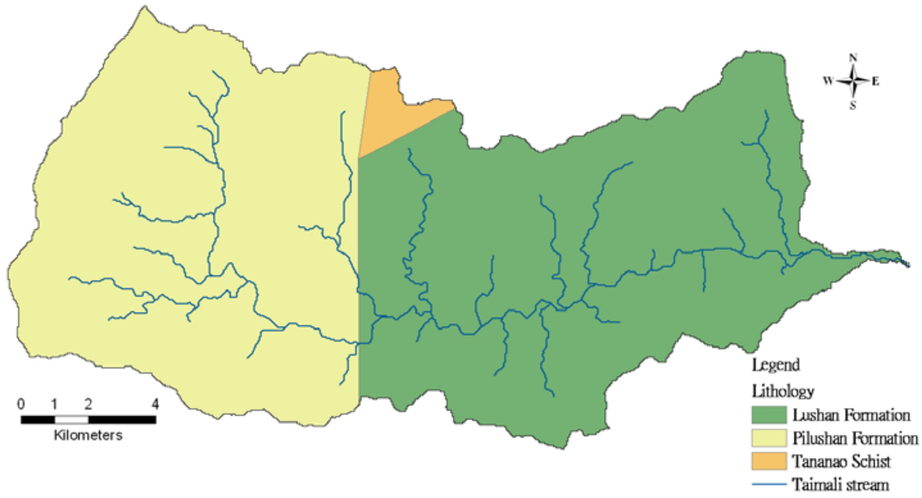

Fig. 3.2 Lithology map

Fig. 3.3 Distance to faults map

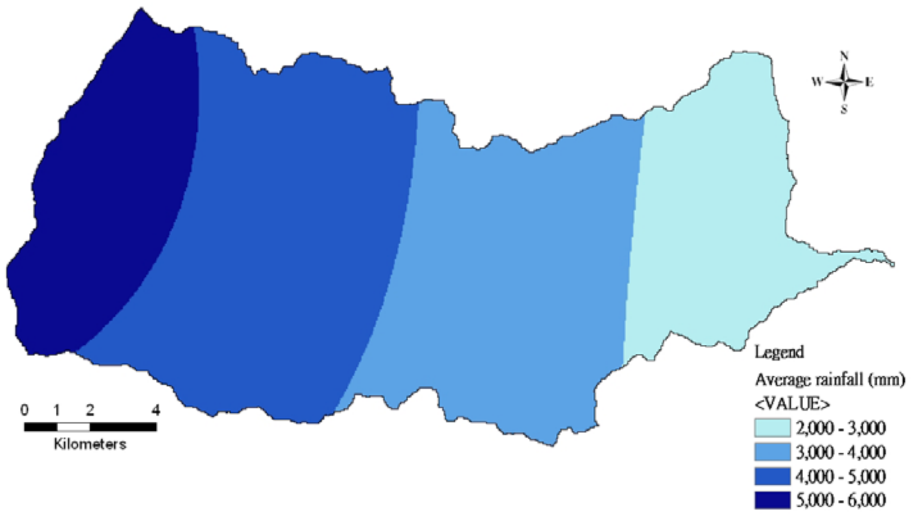

Fig. 3.4 Average annual rainfall map

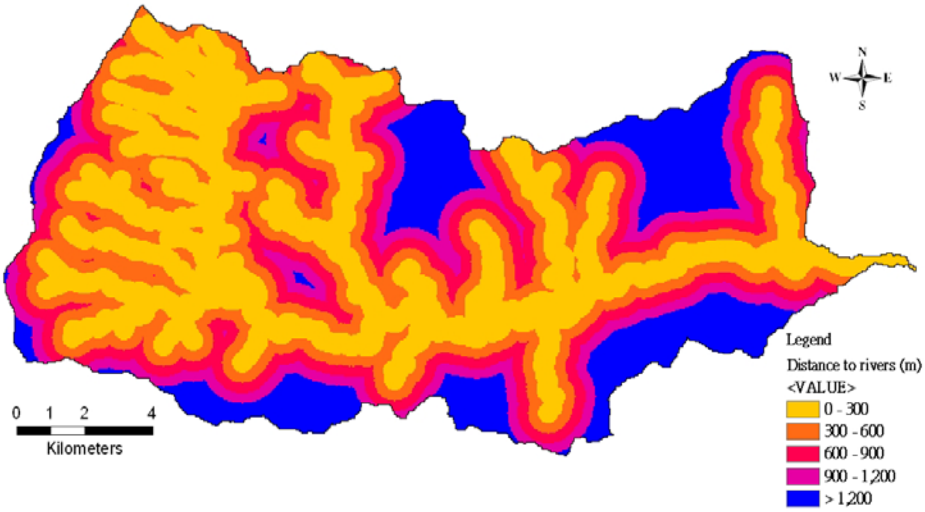

Fig. 3.5 Distance to rivers map

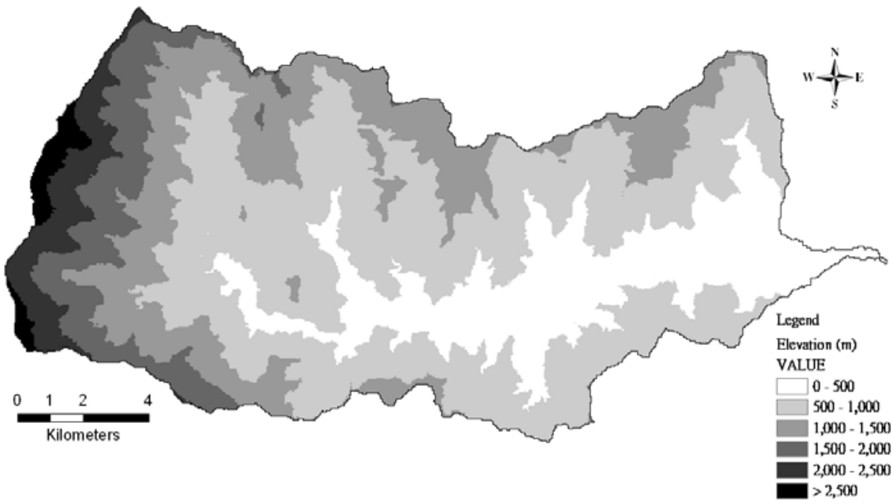

Fig. 3.6 Elevation map

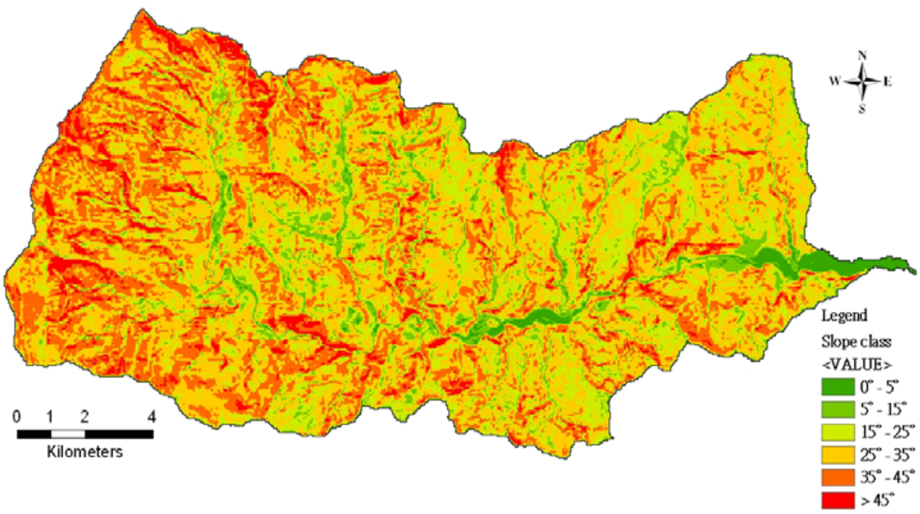

Fig. 3.7 Slope map

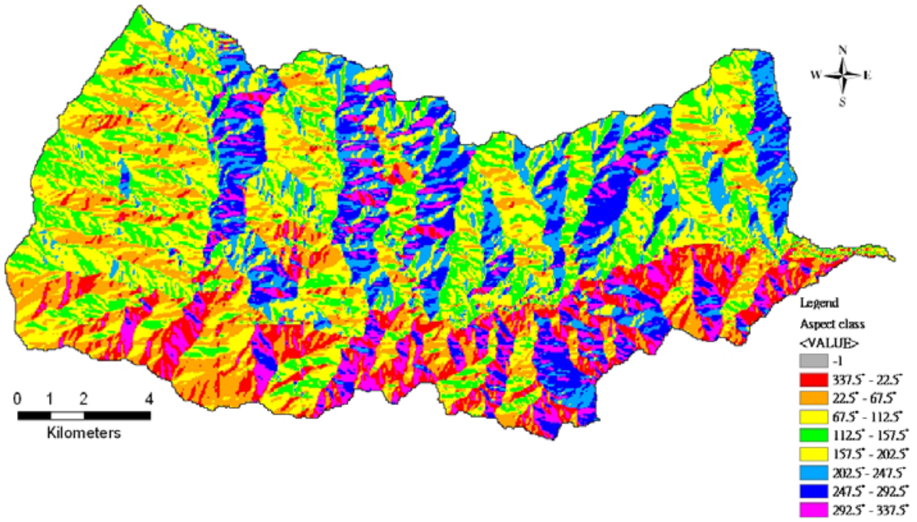

Fig. 3.8 Aspect map

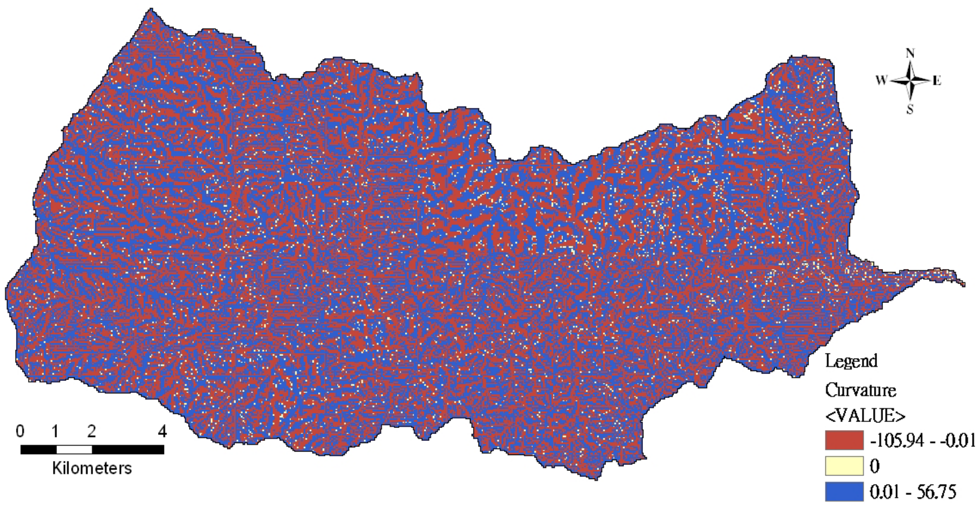

Fig. 3.9 Curvature map

3.6.2 Change analysis in association with environmental variables

(1) Percentage of the entire area of change

The changed area in each subregion of the distribution map of the environmental variables could be computed using the "Tabulate Area" of spatial analyst tools in ArcGIS. Then the changed area in each subregion divided by that of the entire watershed gives rise to the percentage of the entire area of change, which reveals what the percentage of change in each subregion is (Wang et al. 2012).

(2) Relative change intensity (RCI) index

To explicitly quantify the concentration of land cover change in a specific subregion of the entire watershed, the relative change intensity (RCI) index is applied in our study. The concept of RCI, derived from the research of Wang et al. (2012), is analogous to the Location Quotient that is a tool for comparing regional industry composition. The RCI index can be used to understand change intensity in a subregion as compared with that in other subregions or the entire watershed. The RCI value can be calculated by the following equations (Wang et al. 2012):

$$\mathrm{RCI} = \mathrm{Rsc}/\mathrm{Rec} \tag{3.5}$$

$$\mathrm{Rsc} = \mathrm{Asc}/\mathrm{As} \tag{3.6}$$

$$\mathrm{Rec} = \mathrm{Aec}/\mathrm{Ae} \tag{3.7}$$

where RCI can be expressed by the proportion of the change ratio in a subregion Rsc to that in the entire watershed Rec; Rsc equals the proportion of changed area in the subregion Asc to the entire area of the subregion As; Rec equals the proportion of changed area in the entire watershed Aec to the entire area of the watershed Ae. The RCI index has a value of 1 when the change ratio in the subregion equals that in the entire watershed, and it increases when the change ratio in the subregion is larger than that in the entire watershed.

3.7 Logistic regression model

3.7.1 Mathematics of logistic regression

In the present study, we observe some independent variables, such as elevation, slope, aspect, etc., on every pixel for which we have also determine the status of change, as either 1 if "with change" or 0 if "without change". We would like to use these independent variables to estimate the probability that the land cover change will occur for every pixel during a defined study period. Since the dependent variable is a binary variable being 1 versus 0, it would be proper to apply the logistic regression model to describe the probability of change. The logistic regression model, based on the logistic function, can be expressed in the formula (Bai et al. 2010; Kleinbaum and Klein 2010):

$$P(Y = 1) = \frac{1}{1+e^{-z}} \tag{3.8}$$

where P is probability of occurrence of land cover change for every pixel, which ranges between 0 and 1 on a S-shape curve; z can be substituted for the linear sum expression of β_0 plus β_1 times X_1 plus β_2 times X_2, and so on to β_k times X_k:

$$z = \beta_0 + \beta_1 X_1 + \beta_2 X_2 + \cdots + \beta_k X_k \tag{3.9}$$

where β_0, a constant term, is the intercept of the model; β_i (i = 1, 2,…,k) are the slope coefficients of the model; and X_i (i = 1, 2,…,k) are independent variables of interest.

The terms β_0 and β_i in the model representing unknown parameters could be estimated based on the data of variables X_i and Y (status of change) of the pixels. To find the best fitting set of parameters, maximum likelihood (ML) estimation, a preferred estimation method for logistic regression, is used to estimate the parameters in the model.

3.7.2 Data sampling and multicollinearity diagnostics

To maintain the equal ratio of change presence (1)/change absence (0) and decrease the effect of spatial autocorrelation, the sample data of pixels are selected by applying a stratified random sampling technique. The sample sizes are determined by the dependent variables with different sizes of changed area. Three different sample sizes are used for the logistic regression analysis, including ten percent of the total pixels for overall landscape change trajectory (OL), two percent of the total pixels for forest-landslide trajectory (from forest to landslide, FL) and forest-channel trajectory (from forest to channel, FC), and one percent of the total pixels for vegetation recovery (from landslide to forest,VR), respectively.

Model fitting via logistic regression is sensitive to collinearities among the independent variables in the model, which is the same case in linear regression (Hosmer and Lemeshow 2000). Multicollinearity results from strong correlation between independent variables and may result in incorrect signs and magnitudes of regression coefficients for dependent variables, thereby, leading to inaccurate inferences about relations between independent and dependent variables (Frans 2008). The Pearson correlation coefficient is ordinarily used to assess correlation between two variables, but it would not discern the situation where multiple independent variables may be interdependent. However, the Tolerance (TOL) and Variance Inflation Factor (VIF) could be applied to discern multicollinearity in this situation, and they are two important indexes widely used for multicollinearity diagnosis. The TOL is defined as $1-R^2$, where R^2 is the coefficient of determination calculated by regressing each variable on all the other independent variables (Allison 1999). The lower the TOL value, the higher the multicollinearity. The TOL value below 0.2 demonstrates the presence of multicollinearity between independent variables, and the value below 0.1 reveals serious muliticollinearity among them (Menard 2002). The VIF is obtained from the reciprocal of the tolerance, and shows how inflated the variance of the coefficient is, compared to what it would be in the absence of collinearity (Allison 1999). There are no formal cutoff values for TOL and VIF to determine whether multicollinearity is present between variables. Allison (1999) suggests that a TOL value below 0.4, i.e. VIF value above 2.5, may reveal the presence of multicollinearity. In our study, variables with TOL<0.4 and VIF>2.5 are rejected from the logistic regression analysis.

3.7.3 Analysis of model fit

(1) Pseudo-R^2 statistics

The R^2 statistic, also called the coefficient of determination, which represents the proportion of variation in the data accounted for by a linear regression model, is not appropriate for use with the logistic regression model (Hilbe 2009). The pseudo-R^2 statistics are devised by statisticians to be more appropriate for logistic models and have similar properties to the R^2 statistic of linear regression model. Cox & Snell R^2 and Nagelkerke R^2, both of which are a kind of estimate of the pseudo-R^2 value, could indicate how much the variability of the dependent variable may be explained by all included predictor variables (George and Mallery 2010). Ranging from 0 to 1, the higher the Cox & Snell R^2 and Nagelkerke R^2 values, the better the fit of the model. Both pseudo-R^2 statistics are widely used by many researchers (Bai et al. 2010; Bui et al. 2011; Lin et al. 2010) and thus are employed by the present study to assess the model fit.

(2) Classification table

The classification table, summarizing the results of a fitted model, is one of the original fit tests used by statisticians with logistic regression (Hilbe 2009). The classification table is the result of cross-classifying the outcome variable, y, with a dichotomous variable whose values are derived from estimated logistic probabilities (Hosmer and Lemeshow 2000). Each estimated probability is compared to a defined cutoff point whose most commonly used value is 0.5. If the estimated logistic probabilities are greater than 0.5, then we categorize the cases as the value 1 for the independent variable; and if the probabilities are less than 0.5, then we categorize the cases as the value 0. Based on the 2 × 2 classification table, three kinds of probabilities could be estimated. One is what proportion of "changed" sites are correctly classified (sensitivity), another is what proportion of "unchanged" sites are correctly classified (specificity), and the other is what overall percentage is correctly classified. For a study evaluating the discrimination performance of the model derived from logistic regression, Pearce and Ferrier (2000) uses a 2 × 2 classification table to examine the agreement between predictions and actual observations. Therefore, crosstabulating the observed values with the predicted values for the dependent variable helps us determine how well the model identifies changes in the landscape of Taimali watershed.

3.7.4 Model Validation

Implementing a validation for the prediction results is regarded as one of the important and essential study procedures in prediction modeling, and the prediction model and image will have hardly any scientific significance without some kind of validation (Chung and Fabbri 2003). In addition, model validation may be especially important when the fitted model is applied to predict the outcome for future subjects (Hosmer and Lemeshow 2000). To evaluate data mining models, it is important to separate the data into two sets: one with 70 percent of the sample data, for training the model, and one with 30 percent of the sample data, for testing the model.

The accuracy of logistic regression analysis in modeling the probability of land cover change in the Taimali watershed is validated by evaluating the performance of the classification results obtained from the testing data sets, and by computing the AUC values, RCI values, and percentage of the area of observed change trajectories in various classes of probability of change.

(1) ROC analysis

A more detailed description of classification accuracy could be acquired from the area under the ROC (Receiver Operating Characteristic) curve that provides a measure of the logistic regression model's ability to classify cases into one of two groups (Hosmer and Lemeshow 2000). The ROC curve is constructed by calculating multiple sensitivity/specificity pairs and drawing a plot of sensitivity (true positive rate) on the vertical axis versus 1-specificity (false positive rate) on the horizontal axis for all possible cutoff points (Hilbe 2009). The area under the ROC curve (AUC) ranges from 0 to 1 with higher values indicative of better fit. As a general rule, an AUC value above 0.7 is considered acceptable while a value exceeding 0.9 is regarded as an outstanding discrimination (Hosmer and Lemeshow 2000). AUC values of 0.95 and larger are highly unlikely (Hilbe 2009). Since the ROC curve provides a useful way to evaluate the performance of classification results and compare the different models, it is applied to implement the goodness-of-fit assessment of the model. In the present study, the ROC curves are plotted according to the true positive rate of identified change presence and false positive rate of identified change presence, as the values of the cutoff point varied.

(2) Relative change intensity (RCI) index

Relative change intensity (RCI) index could measure the concentration of land cover change in a subregion of the whole watershed; hence the index is also utilized in this section to validate the model performance. The calculation method refers to equation 3.5-3.7.

4. RESULTS

4.1 Landscape metrics analysis

Landscape metrics are used to measure the landscape composition and spatial configuration, and thus analysis of the metrics at any different time point enables the recognition of dynamic changes in the landscape pattern. This study used nine landscape metrics to quantify the landscape pattern, and demonstrates that natural disturbances have exerted a great influence on landscape changes in the Taimali watershed.

4.1.1 Landscape composition changes

Three land cover maps of the study area from the period 2005–2011 were obtained from satellite image classification (as shown in Fig. 4.1). Based on the primary objective of this study, four major land cover types were detected and delineated. By calculating the two class-level composition metrics for each landscape element, both the class area and percentage distribution during 2005–2011 were produced (Table 4.1). As listed in Table 4.1, the CA of the landslide patches rapidly enlarged from 2.08 km^2 in 2005 to 10.68 km^2 in 2008, and further extended to 17.60 km^2 by 2011. In addition, the CA of the channel corridors showed a similar tendency to that of the landslide patches, and extended from 7.51 km^2 in 2005 to 15.05 km^2 in 2011. In contrast, however, the changes in CA for the forest matrix and human-made patches showed a substantial decline. For example, forest covered an area of 198.04 km^2 in 2005, but by 2008 had been reduced to 187.78 km^2, with a further reduction to 177.14 km^2 in 2011. The CA of human-made patches decreased from 3.90 km^2 in 2005 to 1.75 km^2 in 2011.

For the percentage land area (PLAND), forest matrix was found to be the most dominant land cover type in the Taimali watershed over the study period, and its PLAND was maintained at over 83% at all times. Although the forest type was the landscape matrix, its PLAND have decreased to a great extent from 93.62% in 2005 to 88.77% in 2008, and further to 83.74% in 2011. The PLAND of human-made patches also decreased from 1.84% in 2005 to 0.83% in 2011. In contrast, however, the PLAND for both landslide patches and channel corridors showed a considerable increase, particularly for landslide patches, which increased significantly increased from 0.99% in 2005 to 8.32% in 2011. The PLAND of channel corridors increased from 3.55% to 7.11% during the period 2005–2011. In total, the CA of landslide patches and channel corridors expanded 7.5 times (15.52 km^2) and 1.0 times (7.54 km^2), respectively, between 2005 and 2011. However, the CA of forest matrix and human-made patches shrank by 10.6% (20.90 km^2) and 55.1% (2.15 km^2), respectively.

Table 4.1 The area distribution of landscape elements from 2005 to 2011

Elements	2005		2008		2011	
	CA (km^2)	PLAND (%)	CA (km^2)	PLAND (%)	CA (km^2)	PLAND (%)
Landslide patches	2.08	0.99	10.68	5.05	17.60	8.32
Forest matrix	198.04	93.62	187.78	88.77	177.14	83.74
Human-made patches	3.90	1.84	2.48	1.17	1.75	0.83
Channel corridors	7.51	3.55	10.60	5.01	15.05	7.11

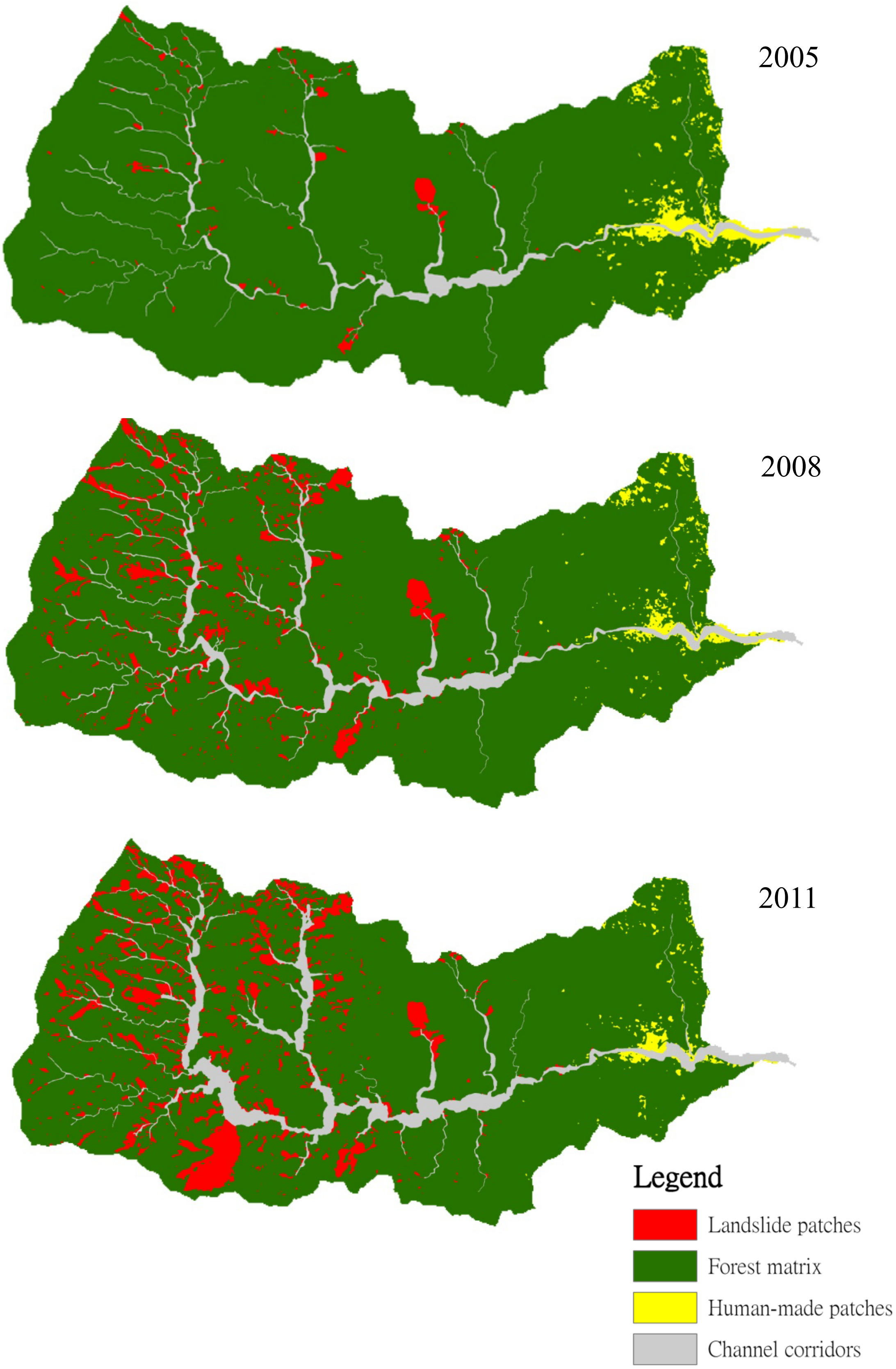

Fig. 4.1 Classified land cover maps of the study area from 2005 to 2011

4.1.2 Spatial configuration changes

By computing seven class-level spatial configuration metrics for each landscape element, the trend in landscape change between 2005 and 2011 was obtained (Fig. 4.2). The patch area is perhaps the single most important and useful piece of information contained in the landscape, and has a large amount of ecological utility in its own right (McGarigal et al. 2012). In addition, the calculation of patch edge provides a valuable measure of the extent of spatial pattern dissection (Cardille and Turner 2002). Edge metrics are even more meaningful when interpreted in combination with other metrics, such as mean patch area (Olsen et al. 2007). NP is also a fundamental metric, and is able to measure the degree of subdivision or fragmentation of a particular patch type (McGarigal et al. 2012). The changes in metrics of AREA_MN, ED, and NP are demonstrated in Fig. 4.2 a–c. In terms of forest matrix, AREA_MN displayed a significant decrease, while ED and NP showed a considerable increment. This suggests that forest fragmentation has created a number of smaller patches with a greater number of dissected edges. In contrast with the forest matrix, channel corridors showed the opposite tendency. Due to their connectivity, the NP of channels was always maintained at 1 throughout the study period. In addition, the increasing AREA_MN and decreasing ED for channels indicates that their patch area expanded and their edges slightly decreased, owing to the expansion of channels in relation to flooding. However, the NP, AREA_MN, and ED for landslide patches all considerably increased over the study period, showing that landslide patches expanded in amount, size, and edge.

Landslides, considered a major sediment source, can supply a large amount of unstable sediment to a basin (Koi et al. 2008). The expansion of landslide patches is related to a series of natural disturbances, and it is considered that this occurrence should receive attention in relation to hazard management. In comparison with values of landslides patches, the values NP, AREA_MN, and ED for human-made patches all decreased gradually, thereby indicating that human-made patches shrank in amount, size, and edge.

Both SHAPE_MN and FRAC_MN measure the complexity of a patch shape. SHAPE_MN has a value of 1 when the patch shape is square and highly compact, and its value increases without an upper limit as the patch shape becomes more irregular (McGarigal et al. 2012). The value of FRAC_MN ranges from 1 to 2, approaching 1 for patch shapes with simple perimeters such as squares or circles, and approaching 2 for patch shapes with highly convoluted perimeters (Mandelbrot 1977). As shown in Fig. 4.2 d and e, both these metrics show a similar trend in change, and the values of both show a decreasing trend for all land cover types except for forest. For forest matrix, SHAPE_MN increased from 1.56 in 2005 to 1.58 in 2011, and FRAC_MN increased from 1.064 in 2005 to 1.072 in 2011. These results suggest that the shape of the forest land cover type became more irregular, but the shape of the other land cover types transformed into more compact and simple shapes.

ENN_MN and AI are applied to measure the extent of isolation and aggregation, respectively, for the patch types. ENN_MN approaches 0 when the distance to the nearest patch of the same type is reduced, and AI ranges from 0 to 100, reaching 100 when the focal patch type is maximally aggregated into a single and compact patch (McGarigal et al. 2012). As shown in Fig. 4.2 f and g, the decreasing ENN_MN but increasing AI for landslide patches indicates that these areas have increasingly become patches of the same type and spatial aggregation. Conversely, increasing ENN_MN and decreasing AI for forest matrix and human-made patches reveals that these two patch types have become more spatially isolated and dispersed. As channel corridors represent only one patch, the ENN_MN of channel corridors could not be defined, and has not been shown in Fig. 4.2 f. However, the AI of channel corridors substantially increased, which reveals an expansion of the spatial aggregation of channel corridors. On the whole, forest matrix patches are shown to have become smaller, more irregular, and more spatially fragmented, isolated, and dispersed. For landslide patches, the values of area, edge, number, and aggregation all showed a gradual increase, but for human-made patches these values showed a decreasing trend. Values of area and aggregation showed an upward trend for channel corridors, but in contrast the values of edge and shape showed a downward trend.

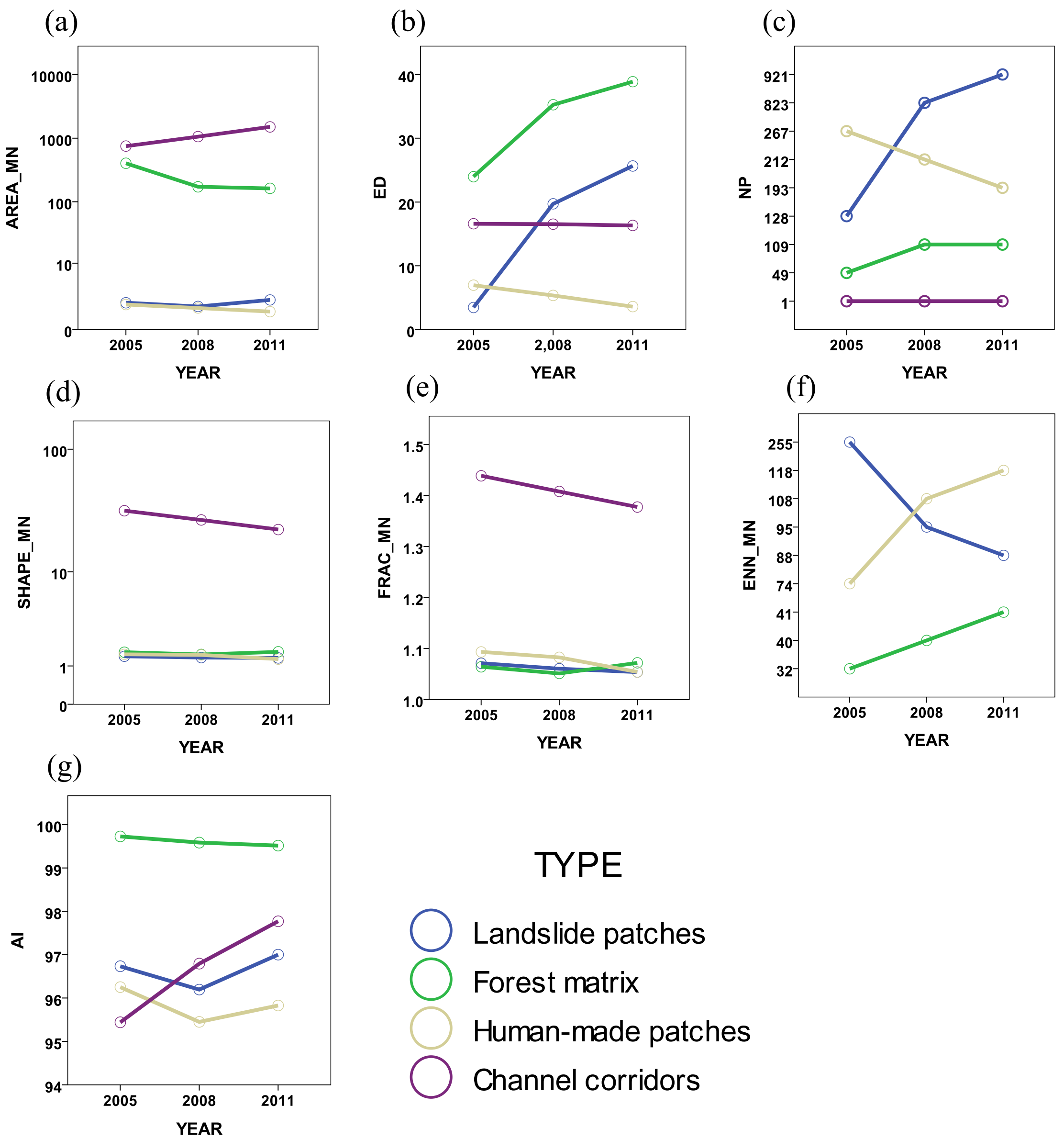

Fig. 4.2 Changes in landscape metrics from 2005 to 2011 (The y-axis is presented on a Log10 scale in Fig. 4.2 a and d)

4.1.3 Summary

Understanding the dynamics of landscape change is helpful to make management plans for the Taimali watershed, which is a representative region in eastern Taiwan susceptible to natural disturbances. In the present study, landscape change refers to not only the change in landscape composition, but also the change in spatial configuration. The identification of change in landscape pattern can be achieved by computing landscape metrics in different time points. Nine landscape metrics at class-level were applied to quantify four landscape elements.

Based on the calculation of CA from 2005 to 2011, the results indicate that the CA of landslide and channel expanded 7.5 times (15.52 km^2) and 1.0 times (7.54 km^2), respectively. However, in the same time period, the CA of forested land and human-made patch shrank 10.6% (20.90 km^2) and 55.1% (2.15 km^2), respectively. As for PLAND, the forest type was found to be the landscape matrix, but its PLAND displayed a great reduction from 93.62% in 2005 to 83.74% in 2011. Besides, the PLAND of human-made patches was also decreasing from 1.84% in 2005 to 0.83% in 2011. On the contrary, the PLAND of landslide patches significantly increased from 0.99% to 8.32%, and the PLAND of channel corridors also showed an increase from 3.55% to 7.11% during the period of 2005-2011.

The seven spatial configuration metrics at class-level can measure a particular patch type about area, edge, number, shape, isolation, and aggregation. Based on the analysis of spatial configuration metrics from 2005 to 2011, the results reveal that forest patches with more edges and numbers were becoming smaller, irregular, and more spatially fragmented, isolated, and dispersed. The values of area, edge, number, and aggregation for landslide patches were all gradually increasing, whereas a decreasing trend of all these values could only be found for human-made patches. This means that landslide patches with more edges and numbers were growing larger and more spatially aggregated. As for channel corridors, the values of area and aggregation had an upward trend, but the values of edge and shape only showed a downward trend.

4.2 Markov chains analysis

Results of landscape metrics analysis show changes in the quantity of landscape composition. It is evident that both the frequency and intensity of typhoons have increased in relation to climate change over recent years, and concerns not only about changes in landscape quantity, but also future changes in trends, are receiving increasing research attention. This section presents the use of Markov chain analysis to describe land cover changes from one point in time to another, in addition to making predictions for future changes.

4.2.1 Area change matrix

Tables 4.2–4.4 show matrices of area change using different time periods. In Table 4.2, the area change matrix shows that the major landscape changes that occurred were forested land replaced by areas of landslides, (over an area of about 8.50 km^2) and by the expansion of channels that encroached on riparian forest (covering an area of about 3.86 km^2). There was therefore a substantial loss of forest cover, measuring 10.26 km^2 (5.2%) between 2005 and 2008. In addition, parts of the human-made patches were converted into forest cover, and these changes probably resulted from farmland being transformed into fallow land or abandoned land and then covered with grass or scrub. These changes are then seen to continue throughout the following time period. As shown in Table 4.3, significant landscape changes occurred in relation to the same events, i.e. landslides patches and channels corridors took the place of forest cover over an area measuring 10.93 km^2 and 4.71 km^2, respectively. However, it is considered that some patches of landslides and channels that were transformed into forest cover could have occurred in relation to the rapid re-vegetation in the humid tropical climate. Overall, between 2005 and 2011, the most remarkable landscape changes occurring under the effects of natural disturbances in the Taimali watershed were the conversion of forest cover into landslides and channels, over areas measuring about 15.82 km^2 and 6.73 km^2, respectively (Table 4.4). In addition, due to farmland abandonment and fallow, the changes from human-made patches into forest cover are also noteworthy.

4.2.2 Transition probability matrix

The transition probability matrix demonstrates the probability of each land cover type converting into another type over a period of time. In this study, transition probabilities were calculated for three time periods: 2005–2008, 2008–2011, and 2005–2011. As shown in Tables 4.2–4.4, the three transition probability matrices all show that the greatest probabilities were for human-made patches changing into forest matrix and channel corridors over the study period. In relation to human-made patches changing into forest matrix, the indication was that farmland converted into fallow or abandoned land would be covered with grasses or scrubs due to re-vegetation. In relation to changes to channel corridors, the indication was that farmland and build-up flooded and flushed away by flood would be changed into channel corridors.

Table 4.2 Matrices of area change (km^2) and transition probability for 2005–2008

2005 data	2008 data							
	Landslide patches		Forest matrix		Human-made patches		Channel corridors	
Landslide patches	1.90	(0.912)	0.09	(0.041)	0.00	(0.000)	0.10	(0.047)
Forest matrix	8.50	(0.043)	184.88	(0.934)	0.81	(0.004)	3.86	(0.020)
Human-made patches	0.00	(0.000)	1.92	(0.492)	1.64	(0.421)	0.34	(0.087)
Channel corridors	0.28	(0.038)	0.90	(0.119)	0.03	(0.004)	6.30	(0.839)

(Numbers in parentheses represent transition probabilities)

Table 4.3 Matrices of area change (km^2) and transition probability for 2008–2011

2005 data	2008 data							
	Landslide patches		Forest matrix		Human-made patches		Channel corridors	
Landslide patches	6.17	(0.578)	3.57	(0.334)	0.00	(0.000)	0.95	(0.089)
Forest matrix	10.93	(0.058)	171.37	(0.913)	0.76	(0.004)	4.71	(0.025)
Human-made patches	0.00	(0.000)	1.12	(0.451)	0.98	(0.394)	0.39	(0.156)
Channel corridors	0.50	(0.047)	1.08	(0.102)	0.01	(0.001)	9.00	(0.850)

(Numbers in parentheses represent transition probabilities)

Table 4.4 Matrices of area change (km^2) and transition probability for 2005–2011

2005 data	2008 data							
	Landslide patches		Forest matrix		Human-made patches		Channel corridors	
Landslide patches	1.67	(0.800)	0.23	(0.111)	0.00	(0.000)	0.18	(0.088)
Forest matrix	15.82	(0.080)	174.96	(0.883)	0.53	(0.003)	6.73	(0.034)
Human-made patches	0.00	(0.000)	1.92	(0.492)	1.22	(0.313)	0.76	(0.195)
Channel corridors	0.11	(0.015)	0.02	(0.003)	0.00	(0.000)	7.37	(0.982)

(Numbers in parentheses represent transition probabilities)

Overall, the second most noticeable transition probabilities occurred between 2005 and 2011 in relation to landslide patches changing into forest matrix and channel corridors (Table 4.4). Changes into forest matrix are in relation to re-vegetation of landslide patches, and conversion to channels corridors in relation to the lateral spread of landslide patches occurring alongside existing channels which are subsequently flooded by sediment to form new expanded channels. The third remarkable transition probabilities occurred in relation to the conversion from forest matrix into landslide patches and channel corridors during the period 2005–2011 (Table 4.4). During 2005–2008, they increased from 0.043 and 0.020, respectively, and during 2008–2011 to 0.058 and 0.025, respectively, with further growth of 0.080 and 0.034, respectively, during 2005–2011. These results suggest that landslides occurring on forested land, induced by natural disturbances, produced a large amount of sediment, and that this sediment then flooded the riparian forest causing the loss of forest cover. Although the probabilities of forest matrix being converted into landslide patches and channel corridors are relatively smaller, they do show the largest amounts of area change, which makes this possibility considerably important.

4.2.3 Predictions of Markov chain

According to the transition probabilities given above, this study utilized Markov chain analysis to predict the next 24 years' percentage distribution of land cover type in the Taimali watershed. As shown in Fig. 4.3, transition probabilities derived from the computation of three different periods gave rise to three statuses of prediction. Under status A, the proportion of forest cover will undergo a dramatic decline from 75.34% in 2017 to 57.55% in 2035. Between 2011 and 2035, the prediction of the decrease in the proportion of forest cover will rise to 26.19%. Human-made patches will also show a considerable reduction in proportion from 0.49% in 2017 to 0.26% in

2035. In contrast however, there will be a large increase in the proportion of landslide patches and channel corridors, from 13.46% and 10.73% in 2017 to 20.65% and 21.57% in 2035, respectively. This status presents a situation where landslides will take place on forested lands, resulting in a forest area reduction and fragmentation. The sediment produced by landslides will then be transported and deposited in channels, and with heavy rainfall the floods will carry sediment downstream to cause inundation of riverine land. Therefore, status A is regarded as presenting a high risk to downstream life and property.

For status B, the predicted result shows that the proportion of forested land will decrease moderately. In addition, channel proportions will expand slightly, while landslide proportions will increase greatly. Overall, the landscape changes in status B will be less than status A, so status B is considered a moderate risk to downstream life and property. For status C, most of the changes in the proportion of each land cover type will be slighter in comparison with status A and B; therefore, status C is regarded as representing a low risk to downstream life and property.

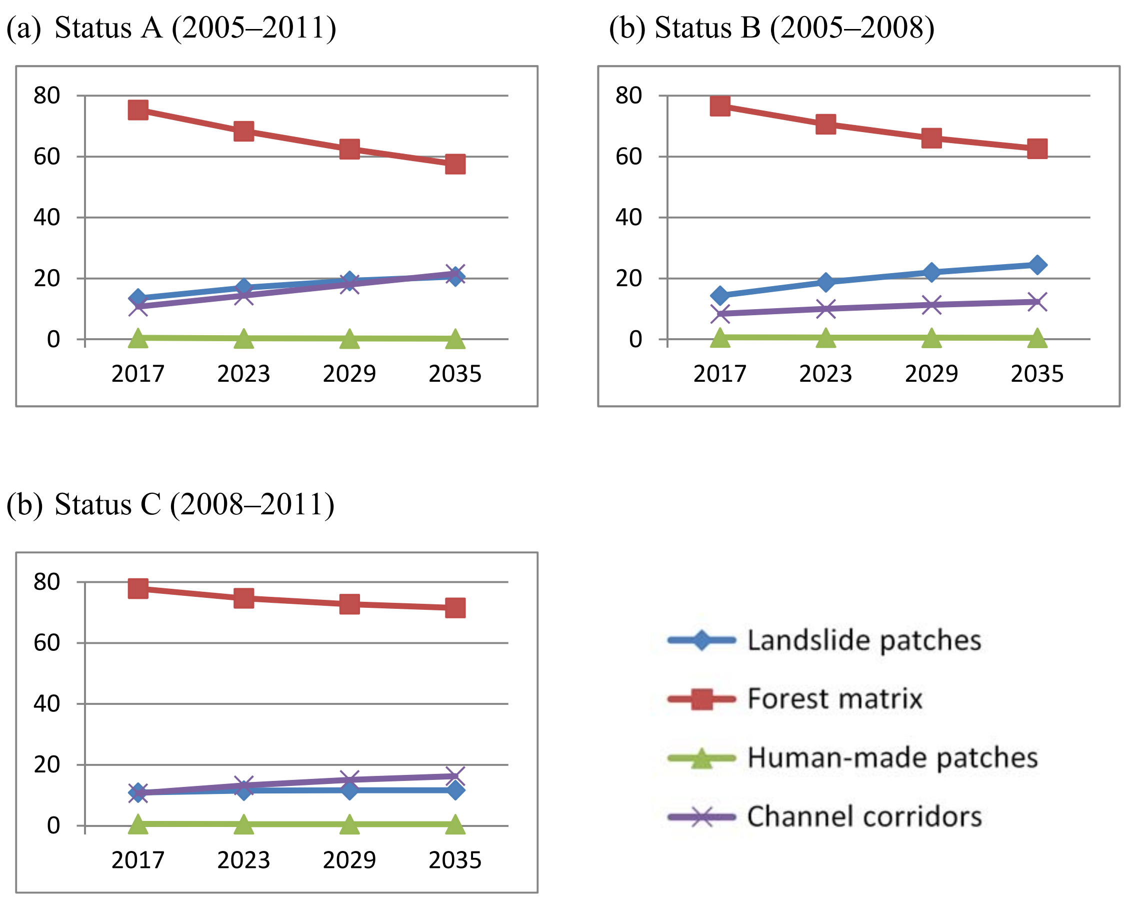

Fig. 4.3 Prediction of land cover changes during 2017–2035 (%)

4.2.4 Summary

After the changes in landscape composition for quantity are recognized, the future trend changes in quantity are the focus of attention in this section. The Markov chain model, a stochastic model, can describe and predict landscape changes without practical measurements of large numbers of factors. When Markov chain analysis are applied for predicting the proportion of each land cover type in the future, both area change matrix and transition probability matrix in land cover type from one time point to another should be built first. The disturbance regime is variable due to disturbances with different sizes, intensities, and frequencies. Thus, transition probability computed from different time periods is regarded as a proxy for variable disturbance regimes to predict future landscape changes under varying statuses of natural disturbance regimes.

On the whole, from 2005 to 2011, the most noticeable area changes influenced by natural disturbances in the Taimali watershed were the transitions from forest cover to landslides and channels about 15.82 km^2 and 6.73 km^2, respectively. The heavy rainfall triggered landslides and the expansion of channels with flood. As far as transition probability is concerned, the probabilities of human-made patches changing into forest cover and channel corridors were the greatest over the study period. The former indicates that farmland affected by disturbances converted into fallow land or abandoned land, both of which were covered with grasses or scrubs owing to vegetation regrowth; the latter shows that farmland and buildup, both of which were flooded or flushed away by flood, changed into channel corridors. In the same period of time, the second remarkable transition probabilities were that landslides changed into forested lands and channels. In addition, although the transformations from forest cover into landslides and channels were the third noticeable transition probabilities, they should receive more attention due to their largest amounts of area change.

By performing Markov chain analysis with three different disturbance regimes, three future (2017–2035) projections of the proportion of each land cover type were produced. The predicted result under status A will display dramatic landscape changes, including a large reduction in the proportion of forest cover and human-made patches and a great increment in the proportion of landslide patches and channel corridors. On the whole, status A, B, and C are considered to be high, moderate, and low risk levels for the safety of downstream life and property, respectively. Since typhoon frequency and intensity seem to be increasing under the influence of global warming in recent years, status A should be paid particular attention in the future.

4.3 Analysis of land cover change trajectories

Land cover change trajectories are traced by codes and classified on the basis of the driving forces of the change. Moreover, rather than consider each land cover trajectory as a unique case, we are interested in grouping trajectories based on their characteristics. This study attempts to find main trajectories to represent the trend of land cover change influenced by natural disturbances at the landscape level. In this section, our study tries to find answers to the following questions:

1. What were the types and extent of land cover change trajectories in the Taimali watershed from 2005 to 2011?
2. Where did the hotspots of land cover change occur?
3. Which environmental variables were associated with land cover change?

4.3.1 Calculation and classification of land cover change trajectories

Trajectory codes are established through formula calculation by applying the raster calculator in ArcGIS 9.3.1. For example, the trajectory of land cover change which converts from forest to landslide, and then to landslide on a pixel over three time points is marked as 211. Theoretically, there will be 64 (4^3) kinds of possible trajectory codes produced; however, practically some trajectory codes do not exist and some take very small percentages of the total study area so they can be omitted. To minimize potential analytic errors, the isolated trajectories are replaced with new values based on the majority of their neighboring cells through the generalization analysis of the majority filter. A total of 44 trajectories were identified, comprising 4 unchanged trajectories and 40 changed trajectories (Fig. 4.4). The selection of the main trajectories in the study area followed the criteria suggested by Mena (2008). The trajectories covering less than 1 percent of the total watershed area were excluded from the following analysis because they might be derived from the artifacts of classification error. The top 7 trajectories, each of which covered more than 1 percent of the total watershed area, were chosen as the main trajectories and shown in Table 4.5. These trajectories, comprising 95.07% of the entire study area, contained two unchanged and five changed trajectories.

First, the single most significant trajectory (222), comprising 80.32% of the landscape, was the persistence of forest cover. The second most important group of trajectories, comprising 11.75% of the landscape, consisted of five change trajectories that were 221, 211, 224, 212, and 244. These five trajectories selected as the main trend changes of land cover in the Taimali watershed contained 75.65% of the entire changed area (Table 4.6). Based on the cause of conversion, change trajectories could be divided into natural-induced or human-induced change classes at level 1. According to the processes of conversion, all of the five natural change trajectories were grouped into three classes at level 2, inclusive of Forest-Landslide (FL), Forest-Channel (FC), and Vegetation Recovery (VR) (Table 4.6 and Fig. 4.5). Human-induced change class involved change trajectories caused by human activities. This class only occupied 2.84% of the entire changed area, so no level 2 class was further divided. It can be seen most land cover transformations in the study area resulted from natural changes induced by catastrophic typhoons. Therefore, typhoons played a pivotal role in the environmental change of the Taimali watershed. These three classes (or trajectories), inclusive of FL, FC, VR, covering 75.65% of the entire changed area, were considered the main trend changes and represented overall landscape (OL) changes in the Taimali watershed.

Based on the characteristic of natural effects, three level 2 classes can be separated into two groups, i.e., a positive and negative change group. For example, FL and FC, occupying 65.35% of the entire changed area, are negative change groups. They demonstrate that forested lands had converted into landslides or channels, which were caused by the torrential rainfall of strong typhoons. However, on the contrary, VR, taking 10.30% of the entire changed area and indicating vegetation recovery on landslides, belongs to a positive change group. From the point of view of soil and water conservation, disturbances mostly caused negative changes in the Taimali watershed, although there were some dispersed vegetation recoveries.

Table 4.5 The top 7 trajectories in the Taimali watershed

Rank	Trajectory code	Percentage (%)	Cumulative percentage (%)
1	222	80.32	80.32
2	221	5.14	85.46
3	444	3.01	88.46
4	211	2.13	90.59
5	224	1.77	92.36
6	212	1.60	93.96
7	244	1.11	95.07

Table 4.6 The percentages of land cover change trajectories

Level 1 class	Level 2 class	Trajectory code	Percentage of the total area	Percentage of the total changed area
Unchanged			84.47	
	Landslide patch	111	0.76	
	Forest matrix	222	80.32	
	Human-made patch	333	0.39	
	Channel corridor	444	3.01	
Natural-induced change			15.09	97.16
	Forest-Landslide (FL)	221	5.14	33.09
		211	2.13	13.68
	Forest-Channel (FC)	224	1.77	11.40
		244	1.11	7.18
	Vegetation Recovery (VR)	212	1.60	10.30
Human-induced change			0.44	2.84

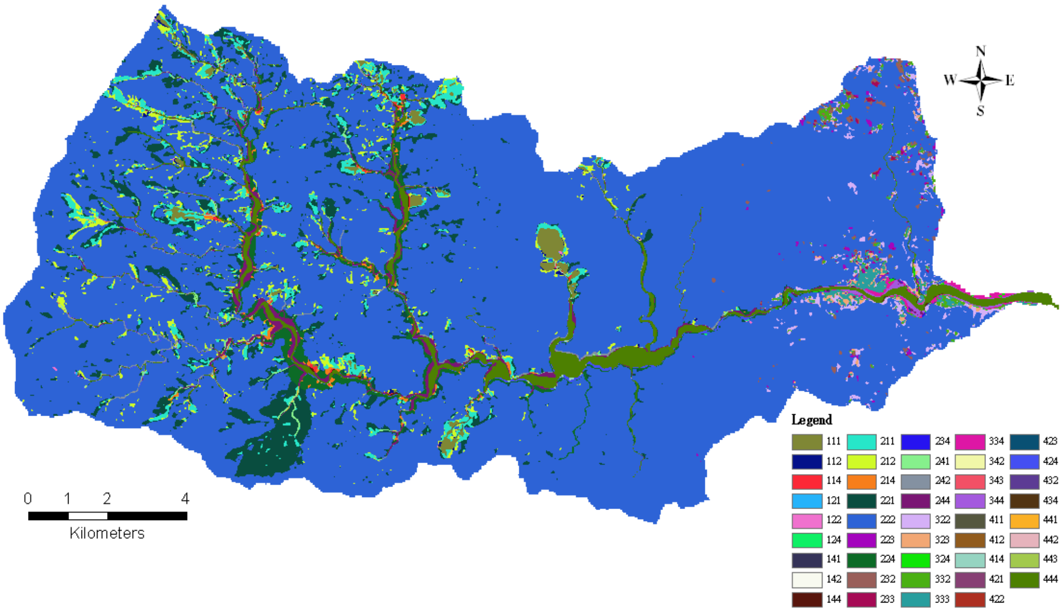

Fig. 4.4 Total trajectories of land cover in the Taimali watershed

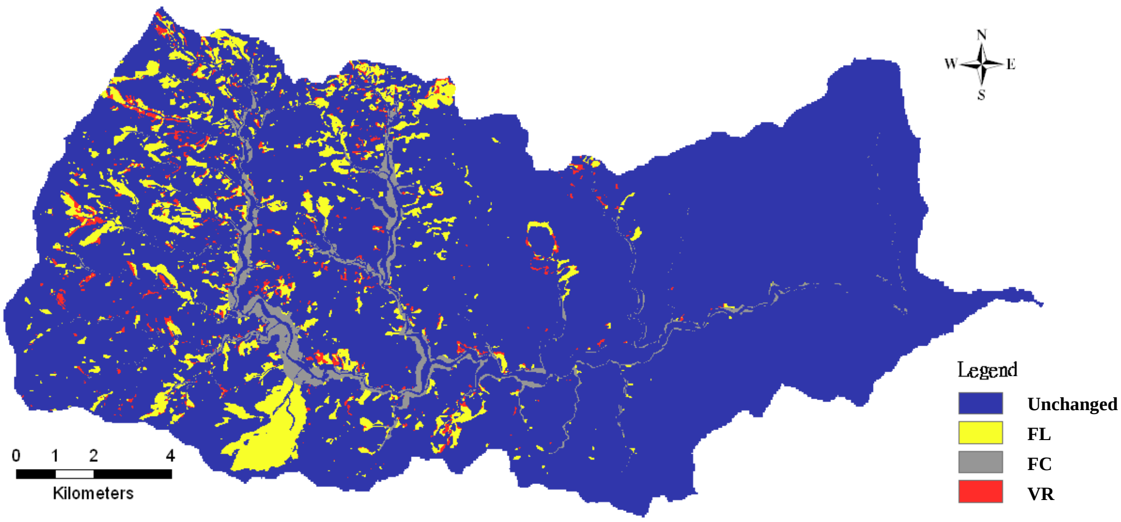

Fig. 4.5 Main land cover change trajectories in the Taimali watershed

4.3.2 Change analysis in connection with environmental variables

After the trajectory layer was acquired, two interesting questions were whether the distribution of change trajectories revealed some spatial characteristics and what environmental variables affected land cover change. To quantify the relationship between the change trajectories and the environmental variables, two steps are necessary. First, the values of selected main change trajectories in the trajectory layer were set at 1 and the values of other unselected trajectories were set at 0. Consequently, a binary map of land cover changes were produced (Fig. 4.6). Second, the binary map was overlaid with the distribution maps of related environmental variables to measure the percentage and RCI of the land cover changes in each subregion of the environmental variables. This analytic process was achieved by carrying out the "Tabulate Area" of spatial analyst tools in ArcGIS. The results of change analysis with the associated eight environmental variables were described as follows:

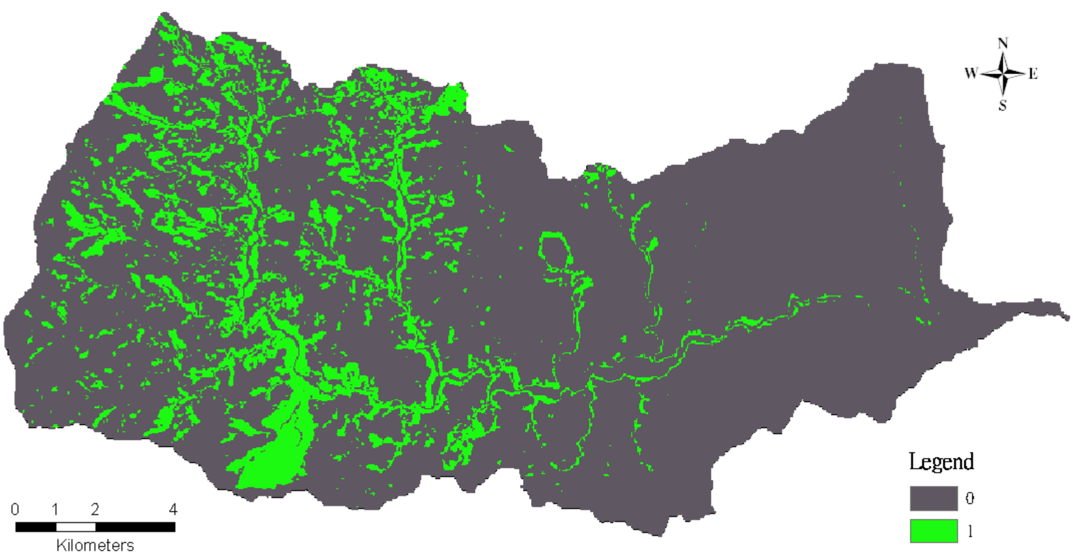

Fig. 4.6 Binary map of land cover trajectories

(1) Lithology

As shown in Table 4.7, two major formations, Pilushan and Lushan, comprise almost the entire watershed and each one covers nearly half of the land area. As presented in Fig. 4.7, RCI values larger than 1 found in the formation of Pilushan and Tananao Schist indicate that there was a highly concentrated land cover change occurring, especially for the Pilushan Formation. Besides, more than 80 percent of the entire changed area was also located in Pilushan Formation. Therefore, it seems that Pilushan Formation is prone to land cover change occurring as a result of relatively fragile geological conditions.

Table 4.7 The area distribution for lithological classes

Class	% Area covered	Area (km^2)	Area of change (km^2)	Change ratio (%)
Pilushan	46.70	98.78	20.33	20.58
Lushan	51.66	109.28	4.06	3.72
Tananao	1.64	3.47	0.51	14.58
Watershed	100.00	211.53	24.90	11.77

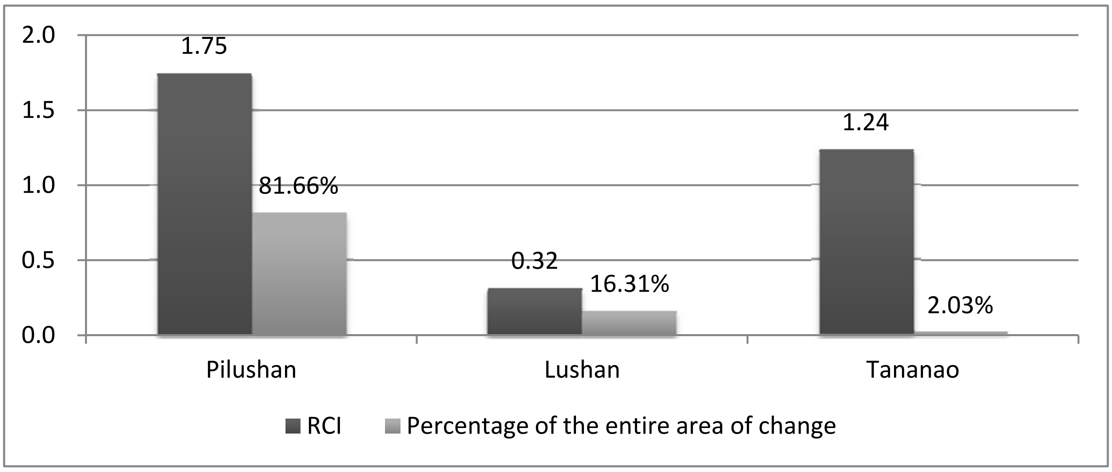

Fig. 4.7 Map of RCI and percentage of the entire area of change for lithology

(2) Distance to faults

Each of the five classes of distance to faults covers about 20% of the study area (Table 4.8). At first, both the values of RCI and percentage of the entire area of change ascended with the increment of distance to faults, and then both of their values showed a decreasing trend when the distance to faults was increasing (Fig. 4.8). Overall, two indexes' values reduced with the increasing distance to faults and this result suggests that the high intensity and large extent of land cover change were situated within 0-6000 m distance to faults. The region adjacent to faults underwent land cover changes to a large extent, probably due to the fragile geologic structure in the neighborhood of the faults.

Table 4.8 The area distribution for classes of distance to faults

Class	% Area covered	Area (km^2)	Area of change (km^2)	Change ratio (%)
0-2000 m	21.05	44.52	6.78	15.23
2000-4000 m	18.86	39.90	6.98	17.48
4000-6000 m	20.54	43.44	5.98	13.77
6000-8000 m	19.51	41.27	3.85	9.33
＞8000 m	20.05	42.41	1.31	3.08
Watershed	100.00	211.53	24.90	11.77

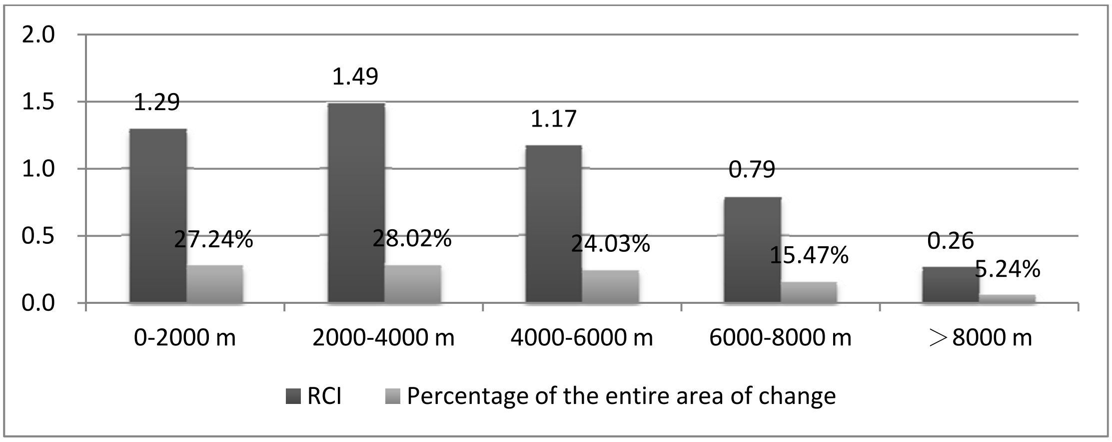

Fig. 4.8 Map of RCI and percentage of the entire area of change for distance to faults

(3) Rainfall

As shown in Table 4.9, the rainfall regions of 4000-5000 mm and 3000-4000 mm take up the two greatest proportions of the study area of about 35% and 30%, respectively. However, the two biggest RCI values were found in the rainfall regions of 4000-5000 mm and 5000-6000 mm with 1.85 and 1.37, respectively (Fig. 4.9). Moreover, the two greatest percentages of the entire area of change were also located in these two regions and the total was up to 88%. These results demonstrate that two regions experienced concentrated and extensive land cover changes. A large amount of rainfall might cause the movement of soil and rocks to trigger landslides and channel expansion.

Table 4.9 The area distribution for rainfall classes

Class	% Area covered	Area (km^2)	Area of change (km^2)	Change ratio (%)
2000-3000 mm	18.06	38.21	0.19	0.49
3000-4000 mm	29.76	62.95	2.80	4.46
4000-5000 mm	34.78	73.56	15.98	21.73
5000-6000 mm	17.40	36.80	5.92	16.09
Watershed	100.00	211.53	24.90	11.77

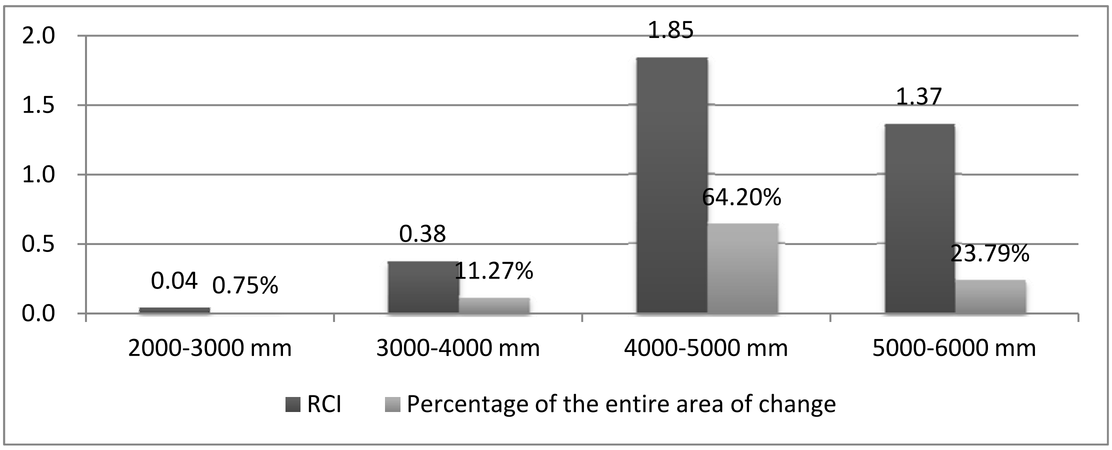

Fig. 4.9 Map of RCI and percentage of the entire area of change for rainfall

(4) Distance to rivers

The change ratios presented a decreasing trend with the increasing distance to rivers (Table 4.10). As illustrated in Fig. 4.10, both the RCI and percentage of the entire area of change displayed a uniform trend where two indexes' values decreased with the increasing distance to rivers. The greatest values of the two indexes were found within 0-300 m distance to rivers and this result reveals that the high intensity and large extent of land cover change were closely adjacent and tied to rivers.

Pearson correlation analysis was performed by regarding distance to rivers as the independent variable and RCI as the dependent variable. The results are presented in Table 4.11 and a scatter plot is also shown in Fig. 4.11. The result of Pearson correlation analysis demonstrates a strong negative linear correlation between distance to rivers and RCI (r = -0.937, Sig. = 0.05). It reveals that the RCI values became smaller when the distance to rivers became larger. The simple linear regression equation is shown below:

$$Y = -0.3516X + 1.8373 \tag{4.1}$$

where Y is the RCI and its value ≥ 0; X is the distance to rivers and its value > 0.

Table 4.10 The area distribution for classes of distance to rivers

Class	% Area covered	Area (km^2)	Area of change (km^2)	Change ratio (%)
0-300 m	35.45	74.99	15.39	20.52
300-600 m	23.21	49.11	5.31	10.81
600-900 m	14.79	31.28	2.21	7.06
900-1200 m	9.69	20.50	1.00	4.88
＞1200 m	16.85	35.65	1.00	2.79
Watershed	100.00	211.53	24.90	11.77

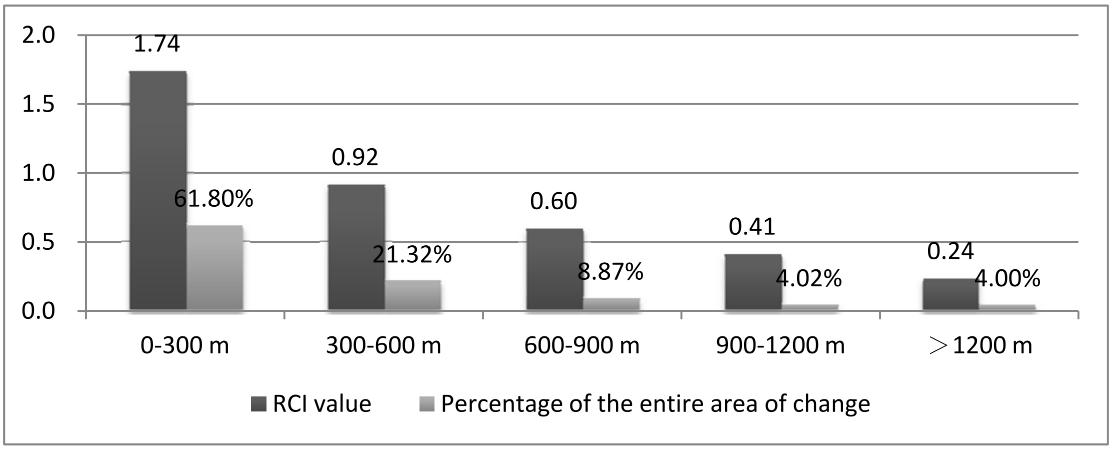

Fig. 4.10 Map of RCI and percentage of the entire area of change for distance to rivers

Table 4.11 Linear correlation analysis between RCI and distance to rivers

		RCI	Distance to rivers
RCI	Pearson correlation	1	-.937*
	Sig. (2-tailed)		.019
	N	5	5
Distance to rivers	Pearson correlation	-.937*	1
	Sig. (2-tailed)	.019	
	N	5	5

* Correlation is significant at the 0.05 level (2-tailed).

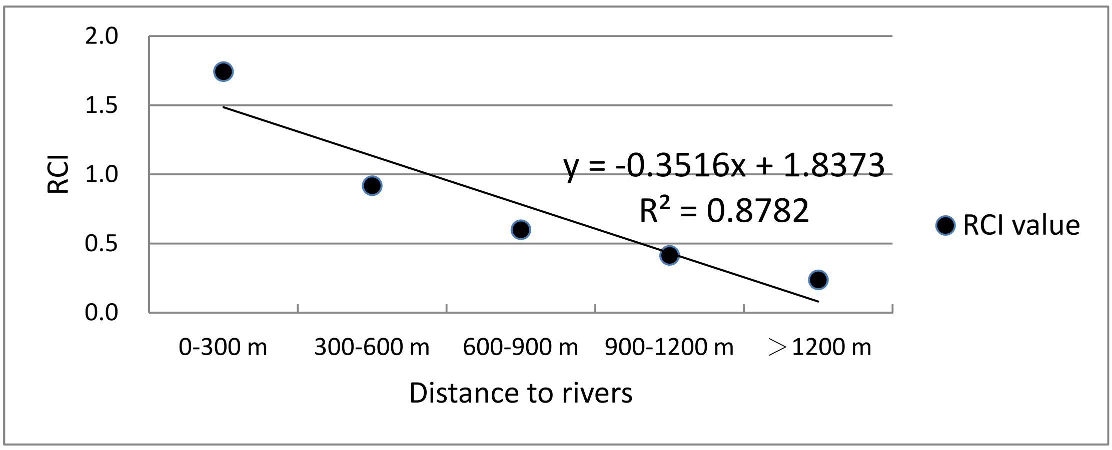

Fig. 4.11 Scatter plot between distance to rivers and RCI value

(5) Elevation

Elevation of 500-1000 m takes up the greatest proportion of area, at about 45%, and the elevation of 0-500 m and 1000-1500 m also occupies considerable proportions, at about 20% and 21%, respectively (Table 4.12). As shown in Fig. 4.12, RCI values larger than 1 demonstrate that there were concentrations of land cover changes at elevations of 1000-2500 m, although the greatest percentage of the entire area of change was found at elevations of 500-1000 m. When explaining the relationship between elevation and land cover change, the correlation between elevation and rainfall and slope should be considered. As a general rule, the higher the elevation is, the greater the rainfall and slope gradient are.

Table 4.12 The area distribution for elevation classes

Class	% Area covered	Area (km^2)	Area of change (km^2)	Change ratio (%)
0-500 m	20.06	42.43	4.42	10.42
500-1000 m	44.79	94.76	9.58	10.11
1000-1500 m	20.82	44.046	6.25	14.20
1500-2000 m	8.35	17.67	3.27	18.51
2000-2500 m	4.45	9.41	1.23	13.02
＞2500 m	1.52	3.22	0.15	4.53
Watershed	100.00	211.53	24.90	11.77

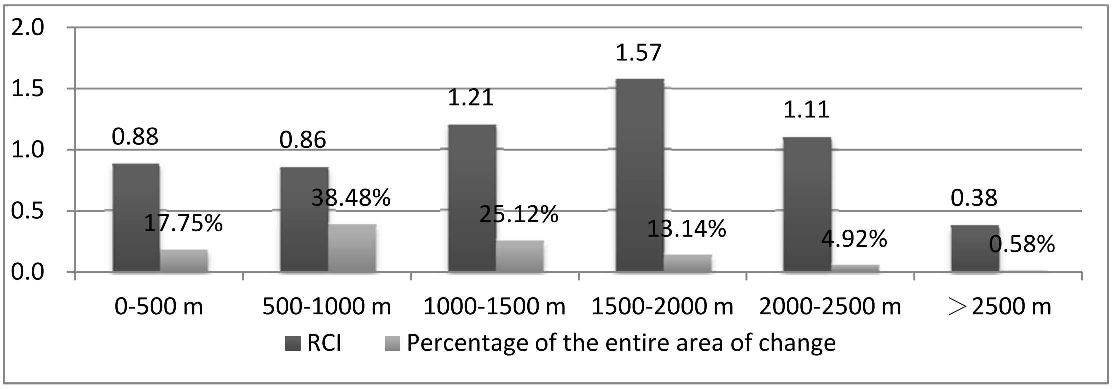

Fig. 4.12 Map of RCI and percentage of the entire area of change for elevation

(6) Slope

The proportions of area covered by slope gradients between 15°-45° are all larger than 21% and the greatest one is located at a gradient of 25°-35° (Table 4.13). Overall, the RCI index increased with the ascending slope grades, but fluctuated at the gradient of 5°-15° (Fig. 4.13). The percentage of the entire area of change also rose with the increasing slope grades, but declined at gradients of 35°-45°. Gradients of 35°-45° and greater than 45°, with the highest RCI values of 1.23 and 1.46 respectively, indicate that land cover had experienced high intensity change in these two subregions. Land cover change may result from forested land becoming landslides on steeper slopes.

Table 4.13 The area distribution for slope classes

Class	% Area covered	Area (km^2)	Area of change (km^2)	Change ratio (%)
0°-5°	1.95	4.13	0.35	8.56
5°-15°	6.87	14.53	1.94	13.36
15°-25°	21.53	45.55	3.88	8.53
25°-35°	39.82	84.23	9.28	11.01
35°-45°	24.84	52.55	7.63	14.51
＞45°	4.99	10.55	1.82	17.22
Watershed	100.00	211.53	24.90	11.77

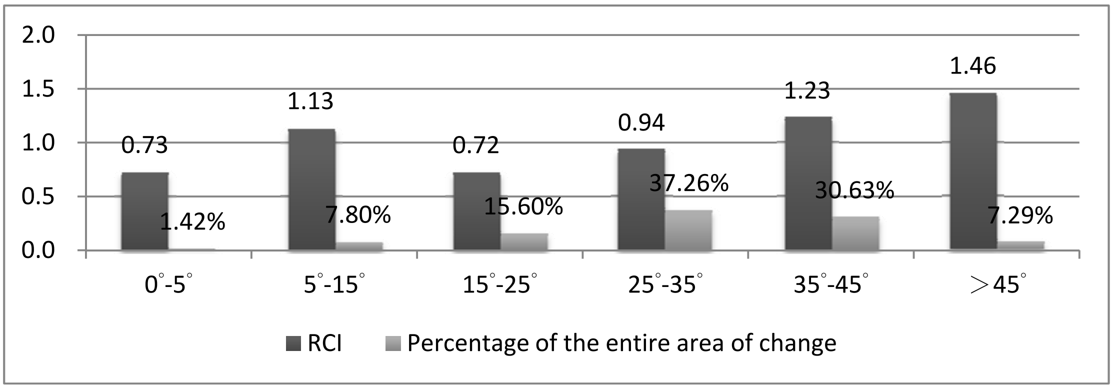

Fig. 4.13 Map of RCI and percentage of the entire area of change for slope

(7) Aspect

The three greatest proportions of area occupied by slope aspects from the northeast, east, to southeast characterize the study area and the total proportion is about 48% (Table 4.14). RCI values greater than 1 were located in the slope of NE, E, SE, and S (Fig. 4.14). The top four percentages of the entire area of change were also situated in the above four slope aspects. Among them, the NE, E, and SE, which occupy 57.09% of the entire area of change, could be grouped into the eastward slope; hence the eastward slope was the dominant region where land cover change occurred. Since the outlet of Taimali watershed is eastward and typhoons often strike Taiwan from the east, typhoons that brought torrential rainfall and wind gave rise to intensive land cover change on the eastward slope.

Table 4.14 The area distribution for slope classes

Class	% Area covered	Area (km^2)	Area of change (km^2)	Change ratio (%)
N	8.90	18.82	1.59	8.43
NE	15.21	32.17	4.50	14.00
E	17.87	37.81	5.36	14.19
SE	14.60	30.89	4.34	14.06
S	12.16	25.73	3.77	14.65
SW	11.73	24.81	2.45	9.87
W	11.40	24.12	1.57	6.51
NW	8.11	17.16	1.31	7.64
F	0.02	0.03	0.00	0.00
Watershed	100.00	211.53	24.90	11.77

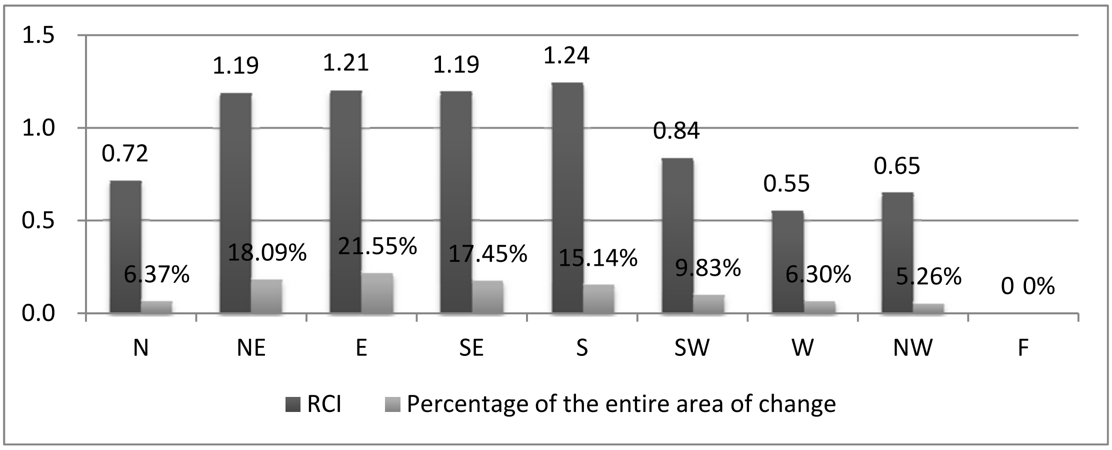

Fig. 4.14 Map of RCI and percentage of the entire area of change for aspect

(8) Curvature

The curvature classes of the study area are primarily comprised of concave and convex landforms that occupy 48% and 49% of the entire watershed, respectively (Table 4.15). As shown in Fig. 4.15, the RCI values in these three subregions of the curvature distribution map were relatively more even than the other environmental variables. RCI values decreased with the negative values transforming into positive ones. The concave area, with a RCI value larger than 1, indicates that higher land cover change intensity occurred in the depression or valley. The greatest percentage of the entire area of change was also found in the concave area but the difference in RCI and percentage of the entire area of change between the concave area and the convex area was not significant.

Table 4.15 The area distribution for curvature classes

Class	% Area covered	Area (km^2)	Area of change (km^2)	Change ratio (%)
Concave (-)	48.00	101.53	13.19	12.99
Flat (0)	2.71	5.74	0.61	10.67
Convex (+)	49.29	104.26	11.10	10.64
Watershed	100.00	211.53	24.90	11.77

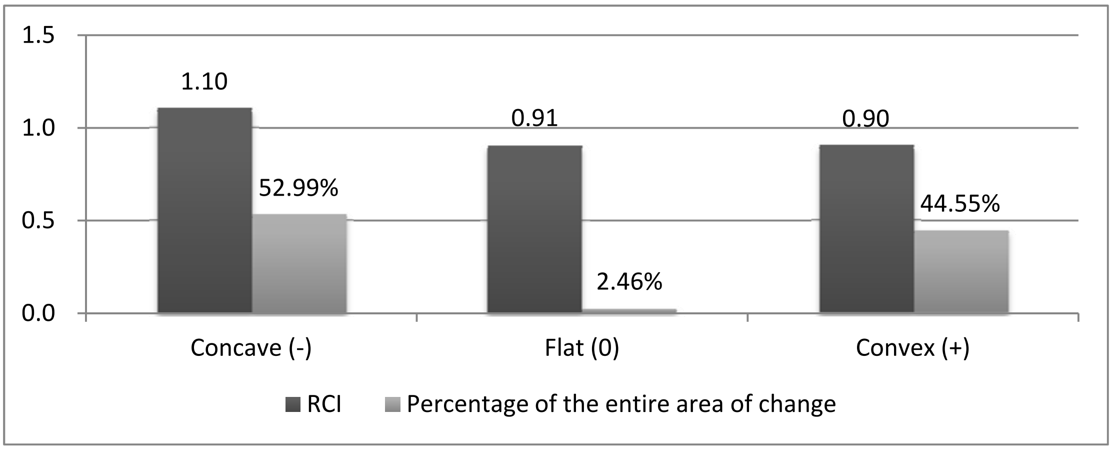

Fig. 4.15 Map of RCI and percentage of the entire area of change for curvature

4.3.3 Summary

Through formula calculation, there were 44 trajectories recognized, inclusive of 4 unchanged trajectories and 40 change trajectories. By referring to selection criteria where the area was larger than 1 percent of the entire study area, the top 7 trajectories were chosen as the main trajectories. These trajectories comprising 95.07% of the entire study area contained two unchanged trajectories and five change trajectories. According to the cause of conversion, five change trajectories belonged to natural-induced change classes at level 1. Based on the processes of conversion, all of the five natural change trajectories were grouped into three classes at level 2, inclusive of FL, FC, and VR. These three classes, covering 75.65% of the entire changed area, were considered main trend changes and represented overall landscape (OL) changes in the Taimali watershed. These results reveal that land cover changes in the study area almost always arose from natural forces. Therefore, natural disturbances play a crucial role in the environmental change of the Taimali watershed. In addition, based on the characteristics of natural effects, three level 2 classes can be divided into two groups, i.e., the positive and negative change group. In terms of soil and water conservation, natural disturbances mostly brought about negative changes in the Taimali watershed, although there were some positive changes of dispersed vegetation recoveries.

To explore the relationship between the change trajectories and the environmental variables, the area of change in each subregion of environmental variables was measured by the percentage of the entire area of change and RCI. The results indicate that a large-area land cover change occurring was subject to the geologic condition of Pilushan Formation and the vicinities of faults and rivers. A great quantity of average annual precipitation, 4000-6000 mm, may lead to the movement of soil and rock to trigger landslides and channel expansion. In addition, land cover experienced highly concentrated changes at elevations of 1000-2500 m, gradients greater than 35°, and on the eastward slope, while the change intensity between the concave and the convex was not significant.

4.4 Logistic regression analysis

To further grasp the relationship between the change trajectories and the environmental variables, we applied logistic regression models and used these eight environmental variables (independent variables) to estimate the probability that the change trajectories (dependent variables) will occur for every pixel. There were four change trajectories, including OL, FL, FC, and VR. Probabilities of change were calculated for four change trajectories, respectively. Before computing the probabilities of change, multicollinearity must be checked to ensure the absence of interdependence. After the fitted logistic models were found, model validation should be implemented to ensure that the fitted models have predictive power for practical applications.

4.4.1 Multicollinearity diagnostics

Multicollinearity is an undesirable situation where the independent variables are interdependent. To detect multicollinearity, indexes of TOL and VIF were used in the present study. The results of multicollinearity diagnostics for four change trajectories were presented below, respectively.

(1) Change trajectories of overall landscape (OL)

When the change trajectory of OL was the dependent variable, the values of both indexes calculated by all eight predictor variables were shown in Table 4.16. Some variables were found to be correlated with others. When the average annual rainfall variable was removed, there was no multicollinearity between the predictor variables (Table 4.17).

Table 4.16 Statistics of multicollinearity diagnostics of all independent variables for change trajectories of OL

Independent variables	Tolerance	VIF
Rainfall	0.125	7.997
Curvature	0.992	1.008
Lithology	0.328	3.047
Distance to faults	0.606	1.650
Distance to rivers	0.520	1.921
Elevation	0.212	4.715
Slope	0.868	1.152
Aspect	0.917	1.091

Table 4.17 Statistics of multicollinearity diagnostics of seven independent variables for change trajectories of OL

Independent variables	Tolerance	VIF
Curvature	0.995	1.005
Lithology	0.656	1.525
Distance to faults	0.870	1.149
Distance to rivers	0.828	1.207
Elevation	0.594	1.683
Slope	0.869	1.151
Aspect	0.917	1.091

(2) Change trajectories from forest to landslide (FL)

When the change trajectory of FL was the dependent variable, the values of both indexes calculated by all eight predictor variables were shown in Table 4.18. Some variables were found to be in correlation with others. When the average rainfall variable was removed, there was no multicollinearity between the predictor variables (Table 4.19).

Table 4.18 Statistics of multicollinearity diagnostics of all independent variables for change trajectories of FL

Independent variables	Tolerance	VIF
Rainfall	0.126	7.929
Curvature	0.986	1.014
Lithology	0.351	2.851
Distance to faults	0.624	1.602
Distance to rivers	0.529	1.889
Elevation	0.218	4.588
Slope	0.901	1.110
Aspect	0.887	1.128

Table 4.19 Statistics of multicollinearity diagnostics of seven independent variables for change trajectories of FL

Independent variables	Tolerance	VIF
Curvature	0.995	1.005
Lithology	0.671	1.490
Distance to faults	0.865	1.155
Distance to rivers	0.879	1.137
Elevation	0.637	1.570
Slope	0.901	1.110
Aspect	0.888	1.126

(3) Change trajectories from forest to channel (FC)

When the change trajectory of FC was the dependent variable, the values of both indexes calculated by all eight predictor variables were shown in Table 4.20. Some variables were found to be correlated with others. When the average rainfall variable was removed, there was no multicollinearity between the predictor variables (Table 4.21).

Table 4.20 Statistics of multicollinearity diagnostics of all independent variables for change trajectories of FC

Independent variables	Tolerance	VIF
Rainfall	0.145	6.883
Curvature	0.980	1.021
Lithology	0.317	3.151
Distance to faults	0.586	1.707
Distance to rivers	0.460	2.173
Elevation	0.258	3.882
Slope	0.867	1.153
Aspect	0.973	1.028

Table 4.21 Statistics of multicollinearity diagnostics of seven independent variables for change trajectories of FC

Independent variables	Tolerance	VIF
Curvature	0.980	1.020
Lithology	0.647	1.544
Distance to faults	0.860	1.163
Distance to rivers	0.675	1.482
Elevation	0.567	1.765
Slope	0.868	1.152
Aspect	0.973	1.028

(4) Change trajectory of vegetation recovery (VR)

When the change trajectory of VR was the dependent variable, the values of both indexes calculated by all eight predictor variables were shown in Table 4.22. Some variables were found to be in correlation with others. When the average rainfall variable was removed, there was no multicollinearity between the predictor variables (Table 4.23).

Table 4.22 Statistics of multicollinearity diagnostics of all independent variables for change trajectories of VR

Independent variables	Tolerance	VIF
Rainfall	0.124	8.091
Curvature	0.983	1.017
Lithology	0.309	3.234
Distance to faults	0.604	1.656
Distance to rivers	0.599	1.669
Elevation	0.205	4.867
Slope	0.876	1.142
Aspect	0.930	1.076

Table 4.23 Statistics of multicollinearity diagnostics of seven independent variables for change trajectories of VR

Independent variables	Tolerance	VIF
Curvature	0.990	1.011
Lithology	0.647	1.545
Distance to faults	0.792	1.263
Distance to rivers	0.845	1.183
Elevation	0.557	1.796
Slope	0.876	1.142
Aspect	0.931	1.074

4.4.2 Model Results

The classification accuracy assessments for all training data sets were calculated by the SPSS software package. The results of classification accuracy assessment for four change trajectories were demonstrated below, respectively.

(1) Change trajectories of overall landscape (OL)

The measure of −2 Log likelihood (−2LL) indicates to what extent the model fits the data, and smaller −2LL values reveal that the model fits the data better (George and Mallery 2010). The −2LL values in the training data set decreased from 11622.574 in step 1 to 10056.432 in step 7 (Table 4.24). Moreover, higher Cox & Snell R^2 and Nagelkerke R^2 values demonstrate a better model fit. Therefore, a better fit of the data with the model could be found in step 7. Of the pixels used to build the model, 3850 of 4670 pixels that were changed are classified correctly. 2855 of 4602 unchanged pixels were classified correctly (Table 4.25). The predicted classification accuracy of the training data set was 82.4% for changed pixels (sensitivity), 62.0% for unchanged pixels (specificity), and 72.3% for the overall predicted accuracy.

As shown in Table 4.26, independent variables with their respective β_i coefficient values obtained from the fittest logistic regression model can be expressed in the following equation:

$$z = 2.8964 - 0.0818\ \mathit{Curvature} - 1.0507\ \mathit{Lithology} - 0.0003\ \mathit{Distance\ to\ faults} - 0.0018\ \mathit{Distance\ to\ rivers} + 0.0007\ \mathit{Elevation} + 0.0064\ \mathit{Slope} - 0.0669\ \mathit{Aspect} \tag{4.2}$$

The map of probability of change for the OL change trajectories was produced by the raster calculator in ArcGIS 9.3.1 using the Eq. 4.2. To acquire the map of classes of probability of change, the adopted method in reference to many researchers is to classify the probability histograms into several classes (Bai et al. 2010; Bui et al. 2011; Nandi and Shakoor 2009). Break values, generated by the method of manual classification, divide the probability map into five classes of likelihood of change: very low (0 – 0.2), low (0.2 – 0.4), medium (0.4 – 0.6), high (0.6 – 0.8), and very high (0.8 – 1.0). The result of the logistic regression model for OL change trajectories was graphically presented in Fig. 4.16.

Table 4.24 Summary of model fit with seven independent variables for overall landscape change

Steps	−2 Log likelihood	Cox & Snell R^2	Nagelkerke R^2
1	11622.574	0.124	0.166
2	10834.944	0.196	0.261
3	10267.547	0.243	0.324
4	10112.348	0.256	0.341
5	10086.161	0.258	0.344
6	10062.668	0.260	0.347
7(final)	10056.432	0.260	0.347

Table 4.25 Classification table based on the logistic regression model for overall landscape change

Observed		Predicted					
		training data set			testing data set		
		Overall landscape		Percentage	Overall landscape		Percentage
		unchanged	changed	Correct	unchanged	changed	Correct
Overall landscape	unchanged	2855	1747	62.0	1295	713	64.5
	changed	820	3850	82.4	356	1584	81.6
Overall Percentage				72.3			72.9

Table 4.26 Regression coefficients and Wald statistics for overall landscape change

	Coefficient(β_i)	Wald	df	Significance
Curvature	-0.081798	22.654	1	0.000
Lithology	-1.050713	376.224	1	0.000
Distance to faults	-0.000286	589.028	1	0.000
Distance to rivers	-0.001799	716.581	1	0.000
Elevation	0.000708	125.154	1	0.000
Slope	0.006404	6.231	1	0.013
Aspect	-0.066895	26.792	1	0.000
Constant	2.896376	473.742	1	0.000

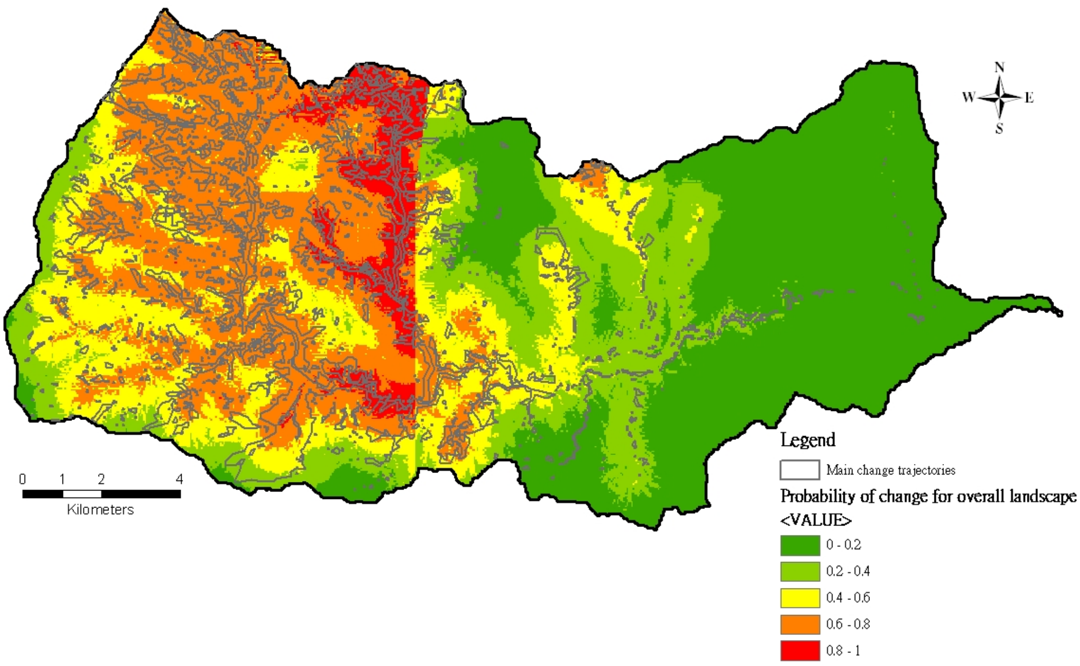

Fig. 4.16 Map of probability of change for OL change trajectories

(2) Change trajectories from forest to landslide (FL)

The −2LL values in the training data set had a reduction from 2271.798 in step 1 to 1965.938 in step 6 (Table 4.27). In addition, higher Cox & Snell R^2 and Nagelkerke R^2 values indicate a better model fit. Therefore, a better fit of the data with the model could be found in step 6. The result of classifying the observations of FL change trajectories using the fitted model was shown in Table 4.28. The overall rate of correct classification of the training data set is estimated as 73.2%, with 84.5% of the changed group and 62.1% of the unchanged group being correctly classified.

As shown in Table 4.29, independent variables with their respective β_i coefficient values that were obtained from the fittest logistic regression model can be expressed by the following equation:

$$z = 1.4922 - 1.1489\ \mathit{Lithology} - 0.0004\ \mathit{Distance\ to\ faults} - 0.0013\ \mathit{Distance\ to\ rivers} + 0.0013\ \mathit{Elevation} + 0.0093\ \mathit{Slope} - 0.0749\ \mathit{Aspect} \quad (4.3)$$

The map of probability of change for FL change trajectories was produced by raster calculator in ArcGIS 9.3.1 using Eq. 4.3. The result of the logistic regression model for FL change trajectories was graphically presented in Fig. 4.17.

Table 4.27 Summary of model fit with six independent variables for forest-landslide change

Steps	−2 Log likelihood	Cox & Snell R^2	Nagelkerke R^2
1	2271.798	0.141	0.188
2	2168.099	0.188	0.251
3	2099.492	0.218	0.291
4	2049.355	0.239	0.319
5	1972.379	0.270	0.360
6(final)	1965.938	0.273	0.364

Table 4.28 Classification table based on the logistic regression model for forest-landslide change

Observed		Predicted					
		training data set			testing data set		
		Forest-landslide		Percentage	Forest-landslide		Percentage
		unchanged	changed	Correct	unchanged	changed	Correct
Forest-landslide	unchanged	574	351	62.1	235	162	59.2
	changed	142	774	84.5	65	341	84.0
Overall Percentage				73.2			71.7

Table 4.29 Regression coefficients and Wald statistics for forest-landslide change

	Coefficient(β_i)	Wald	df	Significance
Lithology	-1.148915	87.896	1	0.000
Distance to faults	-0.000377	142.352	1	0.000
Distance to rivers	-0.001290	86.711	1	0.000
Elevation	0.001288	69.938	1	0.000
Slope	0.039300	36.359	1	0.000
Aspect	-0.074927	6.415	1	0.011
Constant	1.492226	22.555	1	0.000

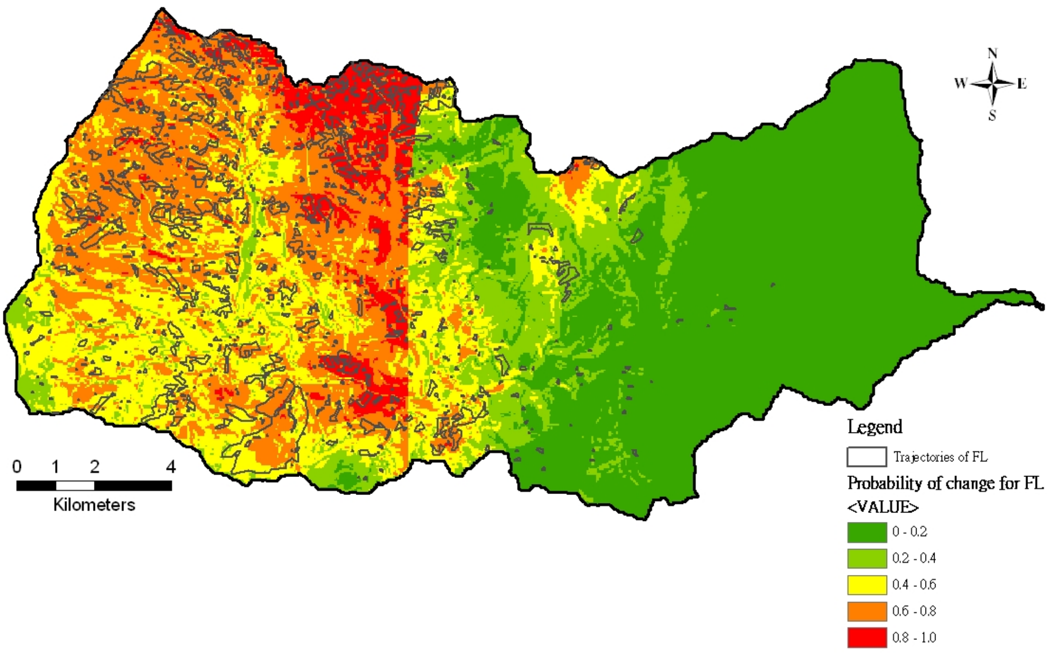

Fig. 4.17 Map of probability of change for FL change trajectories

(3) Change trajectories from forest to channel (FC)

The −2LL values in the training data set had a reduction from 1548.274 in step 1 to 1180.870 in step 5 (Table 4.30). Moreover, higher Cox & Snell R^2 and Nagelkerke R^2 values demonstrate a better model fit. Therefore, a better fit of the data with the model could be found in step 5. The result of classifying the observations of FC change trajectories using the fitted model was shown in Table 4.31. The overall rate of correct classification of the training data set is estimated as 87.9%, with 93.4% of the changed group and 82.3% of the unchanged group being correctly classified.

As shown in Table 4.32, independent variables with their respective β_i coefficient values that were obtained from the fittest logistic regression model can be expressed in the following equation:

$$z = 7.2149 - 1.7534\ Lithology - 0.0002\ Distance\ to\ faults \qquad (4.4)$$

$$- 0.0063\ Distance\ to\ rivers - 0.0029\ Elevation\ - 0.0295\ Slope$$

The map of probability of change for FC change trajectories was produced by the raster calculator in ArcGIS 9.3.1 using the Eq. 4.4. The result of the logistic regression model for FC change trajectories was graphically presented in Fig. 4.18.

Table 4.30 Summary of model fit with five independent variables for forest-channel change

Steps	−2 Log likelihood	Cox & Snell R^2	Nagelkerke R^2
1	1548.274	0.422	0.562
2	1391.180	0.469	0.625
3	1299.481	0.495	0.659
4	1201.129	0.521	0.694
5(final)	1180.870	0.526	0.701

Table 4.31 Classification table based on the logistic regression model for forest-channel change

Observed		Predicted					
		training data set			testing data set		
		Forest-Channel		Percentage	Forest-Channel		Percentage
		unchanged	changed	Correct	unchanged	changed	Correct
Forest-Channel	unchanged	760	163	82.3	331	68	83.0
	changed	61	862	93.4	33	366	91.7
Overall Percentage				87.9			87.3

Table 4.32 Regression coefficients and Wald statistics for forest-channel change

	Coefficient(β_i)	Wald	df	Significance
Lithology	-1.753434	79.102	1	0.000
Distance to fault	-0.000202	43.931	1	0.000
Distance to river	-0.006267	140.957	1	0.000
Elevation	-0.002900	98.058	1	0.000
Slope	-0.029454	20.058	1	0.000
Constant	7.214912	302.392	1	0.000

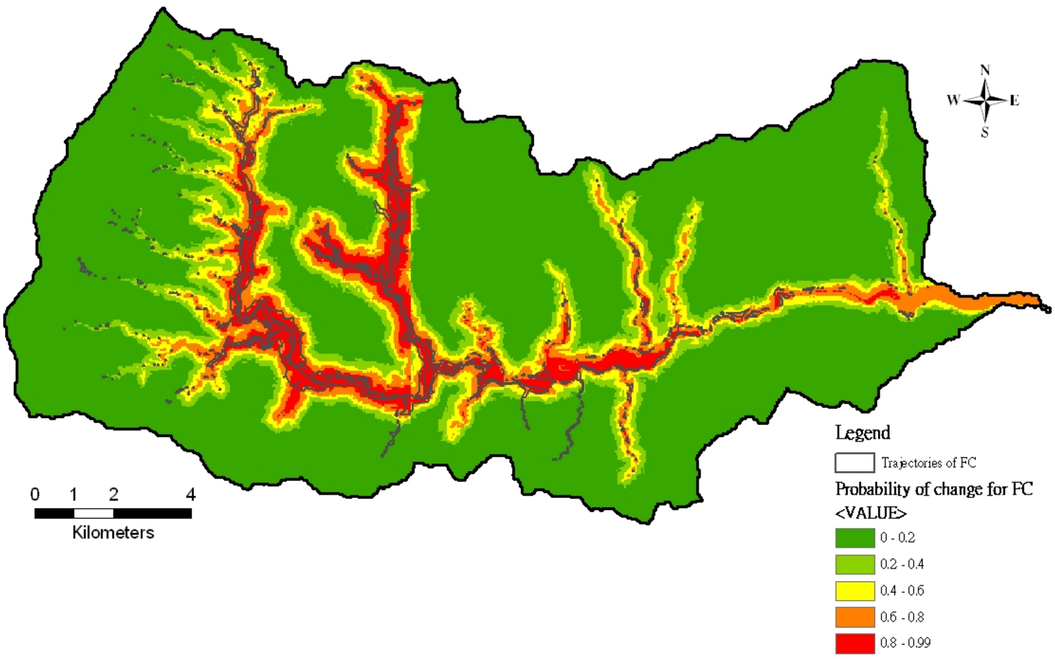

Fig. 4.18 Map of probability of change for FC change trajectories

(4) Change trajectories of vegetation recovery (VR)

The −2LL values in the training data set reduced from 1080.052 in step 1 to 952.354 in step 5 (Table 4.33). Besides, higher Cox & Snell R^2 and Nagelkerke R^2 values reveal a better model fit. Therefore, a better fit of the data with the model could be found in step 5. The result of classifying the observations of VR change trajectories using the fitted model was shown in Table 4.34. Overall, 73.1% of the pixels of the training data set are classified correctly, with 84.6% of the changed group and 60.9% of the unchanged group being correctly classified.

As shown in Table 4.35, independent variables with their respective β_i coefficient values that were obtained from the fittest logistic regression model can be expressed by the following equation:

$$z = 0.9555 - 0.6750\,\textit{Lithology} - 0.0002\,\textit{Distance to faults} - 0.0030\,\textit{Distance to rivers} + 0.0012\,\textit{Elevation} + 0.0287\,\textit{Slope} \quad (4.5)$$

The map of probability of change for VR change trajectories was produced by the raster calculator in ArcGIS 9.3.1 using Eq. 4.5. The result of the logistic regression model for VR change trajectories was graphically presented in Fig. 4.19.

Table 4.33 Summary of model fit with five independent variables for vegetation recovery

Steps	−2 Log likelihood	Cox & Snell R^2	Nagelkerke R^2
1	1080.052	0.180	0.240
2	1026.513	0.227	0.303
3	1002.407	0.247	0.330
4	988.850	0.258	0.345
5(final)	952.354	0.288	0.383

Table 4.34 Classification table based on the logistic regression model for vegetation recovery

Observed		Predicted					
		training data set			testing data set		
		Vegetation recovery		Percentage Correct	Vegetation recovery		Percentage Correct
		unchanged	changed		unchanged	changed	
Vegetation recovery	unchanged	270	173	60.9	148	70	67.9
	changed	72	395	84.6	32	162	83.5
Overall Percentage				73.1			75.2

Table 4.35 Regression coefficients and Wald statistics for vegetation recovery

	Coefficient(β_i)	Wald	df	Significance
Lithology	-0.675009	13.019	1	0.000
Distance to fault	-0.000244	34.526	1	0.000
Distance to river	-0.002977	96.102	1	0.000
Elevation	0.001229	33.191	1	0.000
Slope	0.028693	10.503	1	0.001
Constant	0.955488	5.005	1	0.025

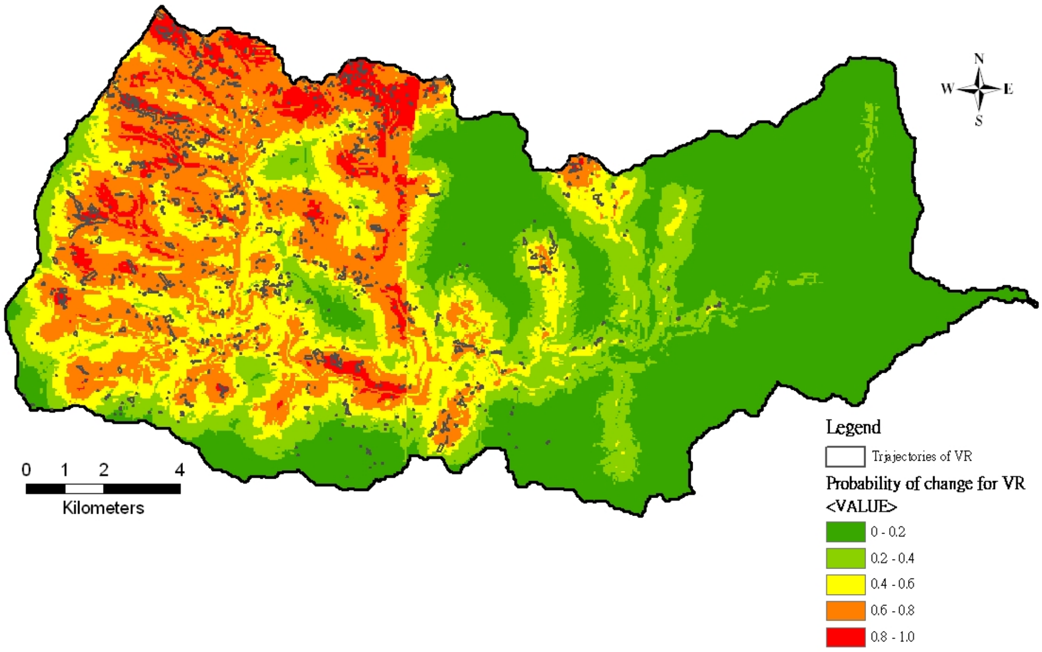

Fig. 4.19 Map of probability of change for VR change trajectories

4.4.3 Model validation

The observed change trajectories of OL, FL, FC, and VR were overlaid on the four corresponding maps of probability of change produced by logistic regression analysis, respectively, and the percentages of area of observed change trajectories located in the five classes of probability of change were calculated. The results of model validation for four change trajectories were demonstrated below, respectively.

(1) Change trajectories of overall landscape (OL)

The predicted classification accuracy of the testing data set is 81.6% for changed pixels and 64.5% for unchanged pixels. Overall, 72.9% of the pixels are classified correctly (Table 4.25). The AUC value of 0.785, which is considered acceptable discrimination, shows that classification results based on the logistic regression model are satisfactory (Fig. 4.20).

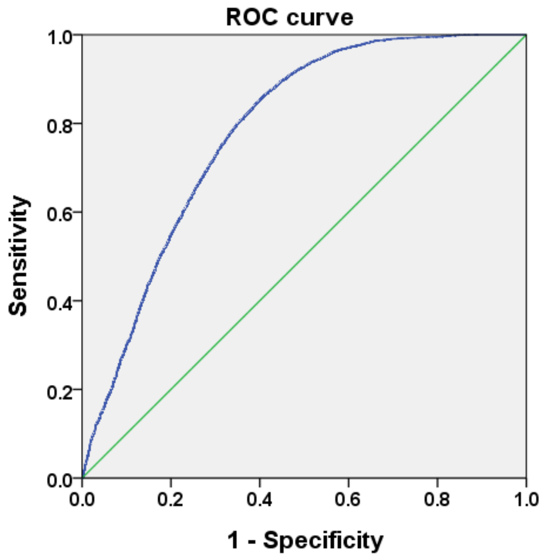

Fig. 4.20 The ROC curve for change trajectories of OL

As for the change trajectories of OL, classes 1 to 5 occupied 32.79%, 17.11%, 18.86%, 25.82%, and 5.43% of the entire study area, respectively (Table 4.36). As shown in Fig. 4.21, the greatest percentage of the entire area of change could be found in class 4. However, as far as the RCI values were concerned, the values were increasing with ascending classes and the greatest value was found in class 5. This result reveals that the observed change trajectories of OL correspond to the zones with higher probabilities of change, which only cover small areas.

Table 4.36 Characteristics of the five classes of probability of change for OL change trajectories

Class number	Probability of change	Propensity to change	% Area covered	Area (km^2)	Area of change (km^2)	Change ratio (%)	RCI	Percentage of the entire area of change
1	0.0–0.2	Very low	32.79	69.37	0.45	0.65	0.06	1.81
2	0.2–0.4	Low	17.11	36.18	2.06	5.70	0.48	8.28
3	0.4–0.6	Medium	18.86	39.89	5.60	14.05	1.19	22.51
4	0.6–0.8	High	25.82	54.61	13.16	24.10	2.05	52.85
5	0.8–1.0	Very high	5.43	11.48	3.62	31.55	2.68	14.56
Total			100.00	211.53	24.90	11.77	1.00	100.00

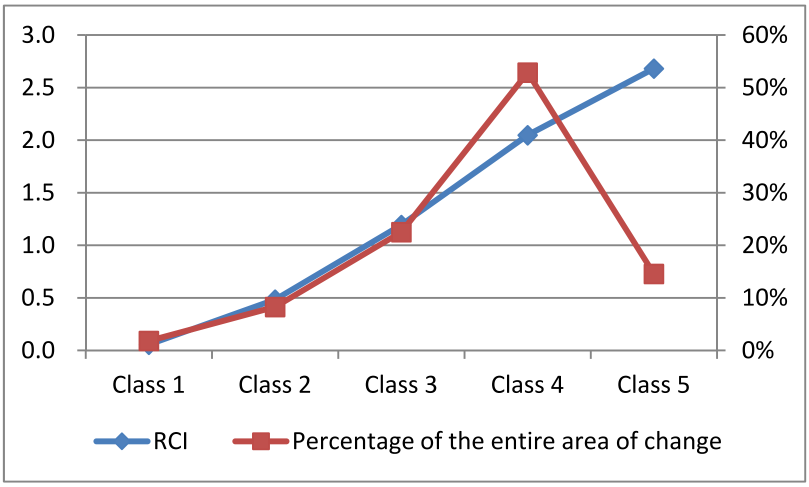

Fig. 4.21 Map of RCI and percentage of the entire area of change for OL change trajectories

(2) Change trajectories from forest to landslide (FL)

The overall rate of correct classification of the testing data set is estimated as 71.7%, with 84.0% of the changed group and 59.2% of the unchanged group being correctly classified (Table 4.28). The AUC value of 0.771, which is also considered acceptable discrimination, indicates that the classification results based on logistic regression model are satisfactory (Fig. 4.22).

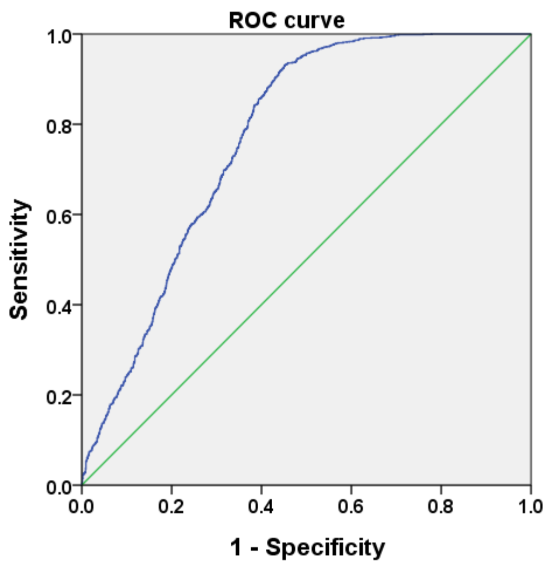

Fig. 4.22 The ROC curve for change trajectories of FL

In regard to the change trajectories of FL, classes 1 to 5 covered 36.81%, 12.81%, 21.29%, 23.09%, and 6.00% of the entire study area, respectively (Table 4.37). As presented in Fig. 4.23, the greatest percentage of the entire area of change could be found in class 4. However, in terms of RCI values, the values showed an increasing trend with rising classes and the greatest value was also found in class 5. This result demonstrates that the observed change trajectories of FL coincide with the zones that have higher probabilities of change and cover a small area.

Table 4.37 Characteristics of the five classes of probability of change for FL change trajectories

Class number	Probability of change	Propensity to change	% Area covered	Area (km^2)	Area of change (km^2)	Change ratio (%)	RCI	Percentage of the entire area of change
1	0.0–0.2	Very low	36.81	77.87	0.24	0.31	0.04	1.56
2	0.2–0.4	Low	12.81	27.11	0.83	3.07	0.42	5.45
3	0.4–0.6	Medium	21.29	45.03	4.68	10.39	1.44	30.62
4	0.6–0.8	High	23.09	48.84	7.24	14.82	2.05	47.35
5	0.8–1.0	Very high	6.00	12.69	2.30	18.09	2.50	15.03
Total			100.00	211.53	15.28	7.22	1.00	100.00

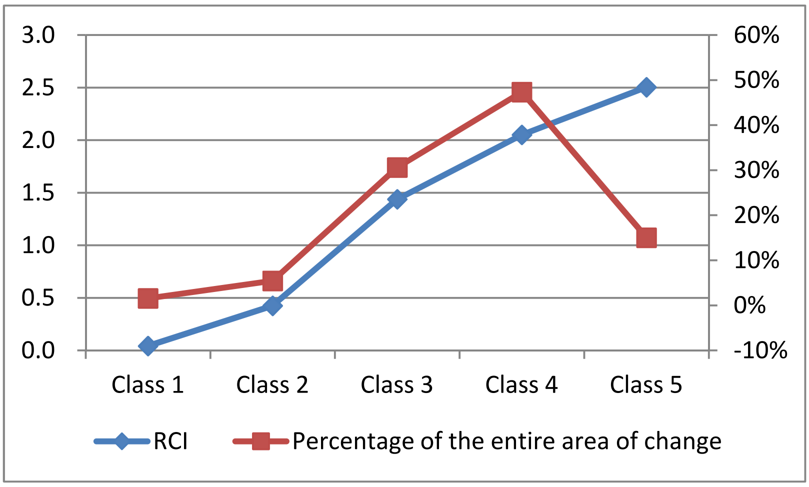

Fig. 4.23 Map of RCI and percentage of the entire area of change for FL change trajectories

(3) Change trajectories from forest to channel (FC)

The overall rate of correct classification of testing data set is estimated as 87.3%, with 91.7% of the changed group and 83.0% of the unchanged group being correctly classified (Table 4.31). An AUC value of 0.941, which is considered outstanding discrimination, indicates that the classification results based on the logistic regression model are very satisfactory (Fig. 4.24).

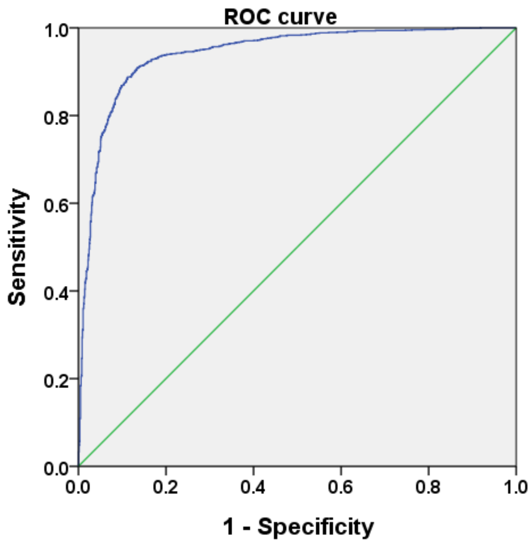

Fig. 4.24 The ROC curve for change trajectories of FC

As for the change trajectories of FC, classes from 1 to 5 comprised 68.63%, 9.86%, 7.46%, 7.73%, and 6.32% of the entire study area, respectively (Table 4.38). As demonstrated in Fig. 4.25, both the greatest RCI value and percentage of the entire area of change could be found in class 5. The two values were increasing with ascending classes. This result is a little different from the two former cases, although it also indicates that the observed change trajectories of FC correspond with the zones, which have higher probabilities of change and cover a small area. A RCI value up to 10.62 is noteworthy and it reveals that the predicted probabilities of change are very spatially accurate.

Table 4.38 Characteristics of the five classes of probability of change for FC change trajectories

Class number	Probability of change	Propensity to change	% Area covered	Area (km^2)	Area of change (km^2)	Change ratio (%)	RCI	Percentage of the entire area of change
1	0.0–0.2	Very low	68.63	145.16	0.29	0.20	0.07	4.68
2	0.2–0.4	Low	9.86	20.86	0.12	0.59	0.20	1.98
3	0.4–0.6	Medium	7.46	15.78	0.24	1.52	0.52	3.86
4	0.6–0.8	High	7.73	16.35	1.39	8.50	2.89	22.34
5	0.8–1.0	Very high	6.32	13.37	4.18	31.26	10.62	67.15
Total			100.00	211.53	6.22	2.94	1.00	100.00

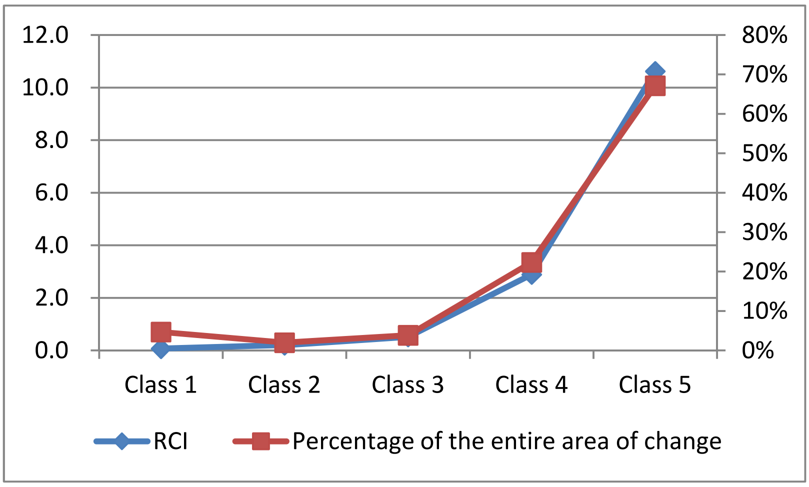

Fig. 4.25 Map of RCI and percentage of the entire area of change for FC change trajectories

(4) Change trajectories of vegetation recovery (VR)

Overall, 75.2% of the pixels of testing data set are classified correctly, with 83.5% of the changed group and 67.9% of the unchanged group being correctly classified (Table 4.34). An AUC value of 0.795, which is also considered acceptable discrimination, indicates that the classification results based on the logistic regression model are satisfactory (Fig. 4.26).

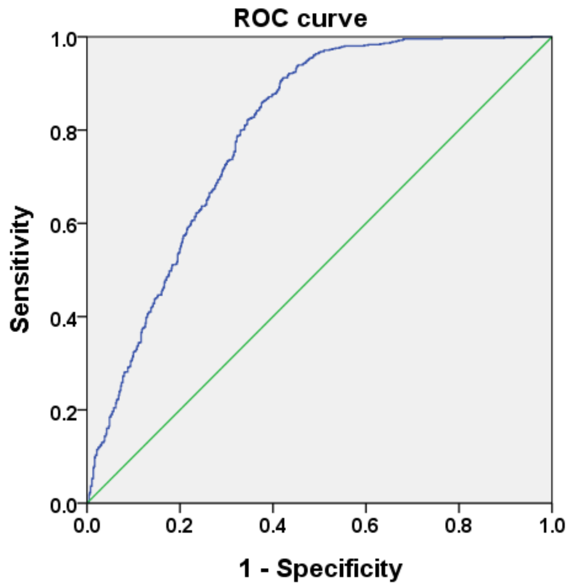

Fig. 4.26 The ROC curve for change trajectories of VR

In terms of the change trajectories of VR, classes 1 to 5 contained 40.18%, 15.64%, 17.93%, 21.45%, and 4.80% of the entire study area, respectively (Table 4.39). As were the cases in the change trajectories of OL and FL, the greatest percentage of the entire area of change and RCI value could be also found in class 4 and 5 in the change trajectories of VR, respectively (Fig. 4.27). RCI values showed an increasing trend with ascending classes. This result indicates that the observed change trajectories of VR match the zones with high probabilities of change and a small area.

Table 4.39 Characteristics of the five classes of probability of change for VR change trajectories

Class number	Probability of change	Propensity to change	% Area covered	Area (km^2)	Area of change (km^2)	Change ratio (%)	RCI	Percentage of the entire area of change
1	0.0–0.2	Very low	40.18	84.99	0.06	0.07	0.04	1.65
2	0.2–0.4	Low	15.64	33.09	0.20	0.60	0.38	5.90
3	0.4–0.6	Medium	17.93	37.93	0.88	2.33	1.45	26.08
4	0.6–0.8	High	21.45	45.37	1.64	3.60	2.25	48.21
5	0.8–1.0	Very high	4.80	10.15	0.62	6.07	3.78	18.16
Total			100.00	211.53	3.39	1.60	1.00	100.00

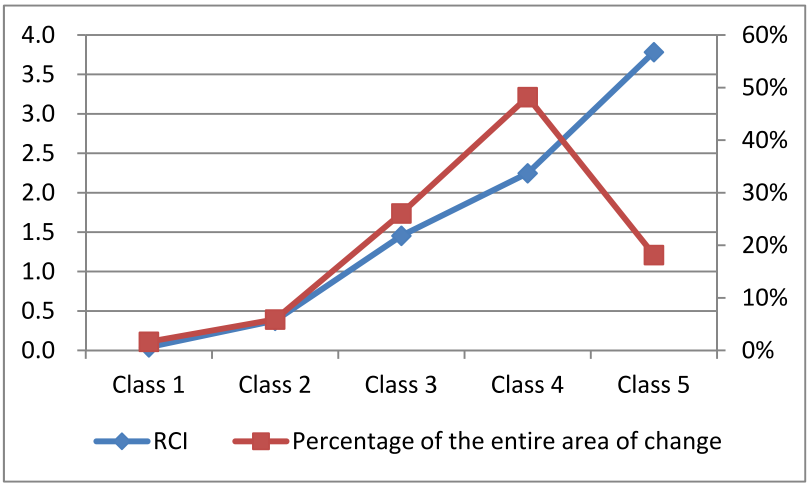

Fig. 4.27 Map of RCI and percentage of the entire area of change for VR change trajectories

4.4.4 Summary

After the relationships between the changed area and environmental variables are understood, knowledge of further predicting the probabilities that change trajectories will occur for every pixel becomes important. Before logistic regression analysis is applied to produce the change probabilities, multicollinearity between predictor variables has to be diagnosed. When the average rainfall variable was removed, there was no multicollinearity between all predictor variables for four change trajectories, inclusive of OL, FL, FC, and VR. With respect to the classification accuracy assessments for four change trajectories, the results demonstrate that the FC model has a better model fit due to its higher Cox & Snell R^2 and Nagelkerke R^2 values and the overall rate of correct classification in the classification table.

By checking the independent variables obtained from the four fittest logistic regression models, five independent variables, including lithology, distance to faults, distance to rivers, elevation, and slope, were all discerned in each logistic regression model. In addition, the aspect variable could be found in OL and FL models, whereas the curvature variable could only be discovered in the former. As regards the signs of regression coefficients for dependent variables, lithology, distance to faults and rivers variables were all negative values in the four models, while elevation and slope variables were all positive values in every model except FL. Concerning the magnitudes of regression coefficients for dependent variables, the coefficient values of the lithology variable were always the largest in the four models and this result revealed that the lithological condition played a crucial role in the four landscape change models. The coefficient values of the aspect variable were the second greatest in the models. When they were absent in the models, the slope variable's coefficient values became the second biggest. These results indicated that aspect and slope variables played a secondary role in the four landscape change models.

As far as model validation was concerned, the FC model had the highest AUC value of 0.941, representing an excellent ability to classify cases into suitable groups, and the other three models also showed acceptable discrimination. Moreover, the RCI values, assessing the intensity of land cover change in a subregion of the entire watershed, showed an increasing trend with the rising classes of change probabilities in the four models and these results suggested that the prediction of change probabilities could very closely correspond with the actual change trajectories. Therefore the four logistic regression models are beneficial tools in landscape change prediction.

5. DISCUSSION

5.1 Assumptions and predictions of Markov chain

This research attempts to show that the Markov chain model is a useful tool for projection, and that it can provide an alternative landscape status for understanding land cover changes over time under different disturbance regimes. The Markov chain model, a distributional landscape model that gives an output of the percentage of land area in a set of classes or element types, cannot deliver sufficient information on the actual location or configuration of land cover types within the landscape, but due to its simplicity and utility it is easier to implement its development and application than using the spatial landscape model (Baker, 1989). In addition, the formation of a landscape pattern is characterized by various interacting factors, while stochastic models (like the Markov chain model) may empirically describe and predict landscape changes with the advantage of saving cost and labor by avoiding practical measurements of large numbers of factors (Balzter, 2000).

To predict future changes in land cover under varying statuses of disturbance regimes, this study uses transition probabilities computed from different time periods as a surrogate for variable disturbance regimes. The predictions of the Markov chain assume that the transition probabilities that occur during three different time periods will remain constant in the future. Thus, three different statuses of prediction are produced to demonstrate the future possible changes in the percentage of land cover types.

Status A predicts extreme changes in the Taimali landscape, and it is therefore hoped that this will be an eventuality. However, researchers have recently become increasingly concerned about the relationship between global warning and typhoon (tropical cyclone) frequency and intensity. Global data reveal a past 30-year trend of more frequent and intense tropical cyclones (Webster *et al.* 2005). Tu *et al.* (2009) found an abrupt shift in typhoon activity in the vicinity of Taiwan. This result indicated that before 2000 (1970–1999) the number of typhoons averaged 3.3 annually, but that the rate grew to 5.7 annually after 2000 (2000–2006). In addition, projection derived from studies of higher resolution modeling showed globally substantial increases in the frequency of the most intense cyclones, and 20% increases in the precipitation rate within 100 km of the storm center (Knutson *et al.* 2010). This worst-case prediction status may be considered to be a little exaggerated, but particular attention should be paid if it occurs in the future.

5.2 Selection of independent variables for logistic models

One of the major goals in this research is to establish exploratory and useful spatial-explicit models of probability of land cover change. Independent variables are selected based on their importance to land cover change and data availability. Logistic regression analyses show that most of independent variables are statistically significant to occurrence of change trajectories. Because predictor variables of this research are relatively easily acquired, it would be beneficial to the application of models in the future. Among the independent variables, average annual rainfall variable is expected to be related to the dependent variable due to the study area within a region of frequent typhoon disturbances. Typhoons may bring a great amount of precipitation to drive changes in land cover. However, rainfall variable is excluded from the resulting logistic models owing to the following two reasons. First, statistics of multicollinearity diagnostics indicates that rainfall variable with the lowest TOL value, *i.e.* the highest VIF value, is strongly correlated with the other variables. When the rainfall variable is attempted to be removed, multicollinearity between the predictor variables is absent. Second, rainfall data are estimated from the surrounding twelve rainfall stations using kriging interpolation technique due to the study area without any of them. However, some stations are a little far away from the study area, hence there is some uncertainty about the estimates.

In addition, annual maximum 1-day and consecutive 3-day precipitation data in 2005, 2009, 2010, respectively, are also estimated from the neighboring twelve rainfall stations using kriging interpolation method to represent extreme precipitation events, which exactly correspond to the typhoons invading Taiwan, namely Typhoon Haitang, Morakot, and Fanipi. Nevertheless, multicollinearity diagnostics also reveals that all annual maximum 1-day and 3-day precipitation variables are highly in correlation with average rainfall variable. Therefore, they are excluded from the resulting logistic models as well.

6. CONCLUSIONS

The landscape changes in the Taimali watershed of eastern Taiwan during 2005-2011 mainly occurred through the loss and fragmentation of forest cover and the increment in the number and area of landslide patches. Many studies on the reduction and fragmentation of forest cover focus on deforestation resulting from anthropogenic activities that are mainly the expansion of agricultural cultivation, the production of commercial timber, and the growth of residential land. However, landscape changes are driven by natural processes and/or anthropogenic activities. The present study revealed that large-scale landscape transformation in the Taimali watershed under the influences of large natural disturbances. Taimali watershed, which is representative of regions of intensive natural disturbances, offers a status suited for studies that enhance our understanding of the complicated interactions between landscape changes and large natural disturbances. To understand landscape changes under the effects of natural disturbances, we took a combined landscape analysis approach that applied landscape metrics, the Markov chain model, change trajectories, and the logistic regression model.

Based on the results and discussion described in this study, the conclusions are as below:

1. Landscape metrics analysis

Composition metrics analysis showed that the CA of landslides expand 7.5 times (15.52 km^2), whereas the CA of forest shrank 10.6% (20.90 km^2) from 2005 to 2011. Moreover, the PLAND of forest cover displayed a great reduction from 93.62% to 83.74%, while the PLAND of landslide patches significantly increased from 0.99% to 8.32% in the same time period.

Spatial configuration metrics analysis indicated that forest patches, with more edges and numbers, were becoming smaller, irregular, and more spatially fragmented, isolated, and dispersed. The values of area, edge, number, and aggregation for landslide patches were all gradually increasing, whereas a decreasing trend in all these values could be found for human-made patches. As for channel corridors, the values of area and aggregation showed an upward trend, but the values of edge and shape only showed a downward trend.

2. Markov chains analysis

From 2005 to 2011, the most noticeable area changes were the transitions from forest cover to landslides and channels of about 15.82 km^2 and 6.73 km^2, respectively. As for transition probability, the probabilities of human-made patches changing into forest cover and channel corridors were greatest over the study period. In the same period of time, the second remarkable transition probabilities were the landslides altering into forested land and channels. In addition, although the transformations from forest cover into landslides and channels were the third noticeable transition probabilities, they should receive more attention due to their largest amounts of area change.

By performing Markov chain analysis, three future (2017–2035) projections of the proportion of each land cover type were produced. The predicted result under status A shows that there are dramatic landscape changes, including a large reduction in the proportion of forest cover and human-made patches and a great increment in the proportion of landslide patches and channel corridors. On the whole, statuses A, B, and C are considered to be a high, moderate, and low risk for the safety of downstream life and property, respectively.

3. The analysis of land cover change trajectories

Through formula calculation, selection and reclassification, three change trajectories, inclusive of FL, FC, and VR, covering 75.65% of the entire changed area, were considered the main trend changes and represented the overall landscape (OL) changes in the Taimali watershed. These results revealed that land cover changes in the study area almost always arose from natural forces.

Change analysis indicated that a large-area land cover change was subject to the geologic condition of Pilushan Formation and the vicinities of faults and rivers. A great quantity of average annual precipitation, 4000-6000 mm, may lead to the movement of soil and rock and trigger landslides and channel expansion. In addition, land cover experienced highly concentrated changes at elevations of 1000-2500 m, gradients greater than 35°, and eastward slopes, while the change intensity between the concave area and the convex area was not significant.

4. Logistic regression analysis

By checking the independent variables obtained from the four fittest logistic regression models, five independent variables, including lithology, distance to faults, distance to rivers, elevation, and slope, were all discerned in each logistic regression model. As regards the signs of the regression coefficients for the dependent variables, lithology, distance to faults and rivers variables were all negative values in the four models, while elevation and slope variables were all positive values in every model except FL. Concerning the magnitudes of regression coefficients for dependent variables, the coefficient values of the lithology variable were always the biggest in the four models. Besides, aspect and slope variables played a secondary role in the four models.

As far as model validation was concerned, FC model had the highest AUC value of 0.941, representing an excellent ability to classify cases into suitable groups, and the other three models also showed acceptable discrimination. Moreover, the RCI values showed an increasing trend with the rising classes of change probabilities in the four models and these results suggested that the prediction of change probabilities could correspond with the actual change trajectories very well. Therefore, the four logistic regression models are helpful tools for landscape change prediction.

REFERENCES

Allison, P. D. (1999). Logistic regression using the SAS system: theory and application. Cary, NC: SAS Institute Inc., p 49-51.

Antwi, E. K., Krawczynski, R., & Wiegleb, G. (2008). Detecting the effect of disturbance on habitat diversity and land cover change in a post-mining area using GIS. *Landscape and Urban Planning, 87*, 22–32.

Baasch, A., Tischew, S., & Bruelheide, H. (2010). Twelve years of succession on sandy substrates in a post-mining landscape: a Markov chain analysis. *Ecological Applications, 20*(4), 1136–1147.

Bai, S. B., Wang, J., Lü, G. N., Zhou, P. G., Hou, S. S., & Xu, S. N. (2010). GIS-based logistic regression for landslide susceptibility mapping of the Zhongxian segment in the Three Gorges area, China. *Geomorphology, 115*, 23–31.

Baker, W. L. (1989). A review of models of landscape change. *Landscape Ecology, 2*(2), 111–113.

Balzter, H. (2000). Markov chain models for vegetation dynamics. *Ecological Modelling, 126*, 139–154.

Benabdellah, B., Albrecht, K. F., Pomaz, V. L., Denisenko, E. A., & Logofet, D. O. (2003). Markov chain models for forest successions in the Erzgebirge, Germany. *Ecological Modelling, 159*, 145–160.

Botequilha Leitão, A., Miller, J., Ahern, J., & McGarigal, K. (2006). *Measuring landscapes: a planner's handbook*. Washington: Island Press, p 48.

Braimoh, A. K., & Vlek, P. L. G. (2005). Land-cover change trajectories in northern Ghana. *Environmental Management, 36*(3), 356–373.

Bui, D., Lofman, O., Revhaug, I., & Dick, O. (2011). Landslide susceptibility analysis in the Hoa Binh province of Vietnam using statistical index and logistic regression. *Natural Hazards, 59*, 1413–1444.

Carmona, A., & Nahuelhual, L. (2012). Combining land transitions and trajectories in assessing forest cover change. *Applied Geography, 32*, 904–915.

Central Weather Bureau (CWB) (2005). *Typhoon warning*. URL: http://rdc28.cwb.gov.tw/data/Warnings/2005/HAITANG/Warnings_alert5.200500000000.pdf

Central Weather Bureau (CWB) (2009). *Typhoon warning*. URL: http://rdc28.cwb.gov.tw/data/Warnings/2009/MORAKOT/Warnings_alert8.200900000000.pdf

Central Weather Bureau (CWB) (2010). *Typhoon warning*. URL: http://rdc28.cwb.gov.tw/data/Warnings/2010/FANAPI/Warnings_alert11.201000000000.pdf

Chang, C. W., Lin, P. S., & Tsai, C. L. (2011). Estimation of sediment volume of debris flow caused by extreme rainfall in Taiwan. *Engineering Geology, 123*, 83–90.

Chu, H. J., Lin, Y. P., Huang, Y. L., & Wang, Y. C. (2009). Detecting the land-cover changes induced by large-physical disturbances using landscape metrics, spatial sampling, simulation and spatial Analysis. *Sensors, 9*, 6670–6700.

Chuang, C. W., Lin, C. Y., Chien, C. H., & Chou, W. C. (2011). Application of Markov-chain model for vegetation restoration assessment at landslide areas caused by a catastrophic earthquake in Central Taiwan. *Ecological Modelling, 222*, 835–845.

Chung, C. F., & Fabbri, A. G. (2003). Validation of spatial prediction models for landslide hazard mapping. *Natural Hazard, 30*, 451–472.

Domon, G., & Bouchard, A. (2007). The landscape history of Godmanchester (Quebec, Canada): two centuries of shifting relationships between anthropic and biophysical factors. *Landscape Ecology, 22*, 1201-1214.

Dramstad, W. E., Olson, J. D. & Forman, R. T. T. (1996). *Landscape ecology principles in landscape architecture and land-use planning*. Washington: Island Press. p 14.

Florinsky, I. V. (2012). *Digital terrain analysis in soil science and geology*. Oxford: Elsevier. p 9–10.

Forman, R. T. T. (1995). *Land mosaics: the ecology of landscapes and regions*. Cambridge: Cambridge University Press. p 359.

Frans, L. M. (2008) Estimating the probability of elevated nitrate concentrations in ground water in Washington State. U.S. *Geological Survey Scientific Investigations Report*, 2008–5025, 22 p.

Frondoni, R., Mollo, B., & Capotorti, G. (2011). A landscape analysis of land cover change in the Municipality of Rome (Italy): spatio-temporal characteristics and ecological implications of land cover transitions from 1954 to 2001. *Landscape and Urban Planning, 100*, 117–128.

George, D. & Mallery, P. (2010). *SPSS for windows step by step: a simple guide and reference, 17.0 update*. 4th edition. Boston: Pearson, p 328–329.

Cardille, J. A., & Turner, M. G. (2002). Understanding landscape metrics I. In: Gergel, S. E., & Turner, M. G. (Eds.), *Learning landscape ecology: a practical guide to concepts and techniques*. New York: Springer-Verlag, p 91.

Gustafson, E. J. (1998). Quantifying landscape spatial pattern: what is the state of the art? *Ecosystems,1*, 143–156.

Hietel, E., Waldhardt, R., & Otte, A. (2004). Analysing land-cover changes in relation to environmental variables in Hesse, Germany. *Landscape Ecology, 19*, 473–489.

Hilbe, J. M. (2009). *Logistic regression models*. London: Chapman & Hall/ CRC Press, p 254–258.

Ho, C. S. (1986). *An introduction to the geology of Taiwan: explanatory text of the geologic map of Taiwan*. Taipei: Central geological survey, MOEA, R.O.C, p 57–61. (In Chinese).

Hong, N. M., Chu. H. J., Lin, Y. P., & Deng, D. P. (2010). Effects of land cover changes induced by large physical disturbances on hydrological responses in Central Taiwan. *Environmental Monitoring and Assessment, 166*, 503–520.

Hosmer, D.W., & Lemeshow, S. (2000). *Applied logistic regression*. 2nd edition. New York: John Wiley & Sons, p156–162.

Huang, M. H., Dreger, D., Bürgmann, R., Yoo, S. H., & Hashimoto, M. (2013). Joint inversion of seismic and geodetic data for the source of the 2010 March 4, M_w 6.3 Jia-Shian, SW Taiwan, earthquake. *Geophysical Journal International, 193*, 1608–1626.

Kintz, D. B., Young, K. R., & Grews-Meyer, K. A. (2006). Implications of land use/land cover change in the buffer zone of a national park in the tropical Andes. *Environmental Management, 38*(2), 238–252.

Kleinbaum, D. G., & Klein, M. (2010). *Logistic regression: a self-learning text*. New York: Springer-Verlag. p 4–8.

Knutson, T. R., McBride, J. L., Chan, J., Emanuel, K., Holland, G., Landsea, C., Held, I., Kossin, J. P., Srivastava, A. K., & Sugi, M. (2010). Tropical cyclones and climate change. *Nature Geoscience, 3*, 157–163.

Koi, T., Hotta, N., Ishigaki, I., Matuzaki, N., Uchiyama, Y., & Suzuki, M. (2008). Prolonged impact of earthquake-induced landslides on sediment yield in a mountain watershed: The Tanzawa region, Japan. *Geomorphology, 101*, 692–702.

Lin, Y. P., Chang, T. K., Wu, C. F., Chiang, T. C., & Lin, S. H. (2006). Assessing impacts of typhoons and the Chi-Chi earthquake on Chenyulan watershed landscape pattern in central Taiwan using landscape metrics. *Environmental Management, 38*(1), 108–125.

Lin, Y. P., Chu, H. J., Wang, C. L., Yu, H. H., & Wang, Y. C. (2009). Remote sensing data with the conditional Latin hypercube sampling and geostatistical approach to delineate landscape changes induced by large chronological physical disturbances. *Sensors, 9*, 148–174.

Lin, Y. P., Chu, H. J., & Wu, C. F. (2010). Spatial pattern analysis of landslide using landscape metrics and logistic regression: a case study in Central Taiwan. *Hydrology and Earth System Sciences Discussions, 7*, 3423–3451.

Logofet, D. O., & Lesnaya, E. V. (2000). The mathematics of Markov models: what Markov chains can really predict in forest successions. *Ecological Modelling, 126*, 285–298.

Malaviya, S., Munsi, M., Oinam, G., & Joshi, P. K. (2010). Landscape approach for quantifying land use land cover change (1972–2006) and habitat diversity in a mining area in Central India (Bokaro, Jharkhand). *Environmental Monitoring and Assessment, 170*, 215–229.

Mandelbrot, B. B. (1977). *Fractals: form, chance and dimension*. San Francisco: W.H. Freeman and Company.

McGarigal, K., Cushman, S.A., & Ene, E. (2012). FRAGSTATS v4: Spatial Pattern Analysis Program for Categorical and Continuous Maps. Computer software program produced by the authors at the University of Massachusetts, Amherst. Available on: http://www.umass.edu/landeco/research/fragstats/fragstats.html

Mena, C. F. (2008). Trajectories of land-use and land-cover in the Northern Ecuadorian Amazon: Temporal composition, spatial configuration, and probability of change. *Photogrammetric Engineering & Remote Sensing, 74*(6), 737–751.

Menard, S. (2002). *Applied logistic regression analysis*. 2nd edition. Thousand Oaks, CA: Sage Publications, Inc., p 76.

Mertens, B., & Lambin, E. F. (2000). Land-cover-change trajectories in Southern Cameroon. *Annals of the Association of American Geographers, 90*(3), 467–494.

Miliaresis, G. C. (2008). Quantification of terrain processed. In: Zhou, Q., Lees, B., & Tang, G. A. (Eds.), *Advances in digital terrain analysis*. Berlin Heidelberg: Springer-Verlag, p. 16–17.

Muller, M. R., & Middleton, J. (1994). A Markov model of land-use change dynamics in the Niagara Region, Ontario, Canada. *Landscape Ecology, 9*(2), 151–157.

Munsi, M., Malaviya, S., Oinam, G., & Joshi, P. K. (2010). A landscape approach for quantifying land-use and land-cover change (1976–2006) in middle Himalaya. *Regional Environmental Change, 10*, 145–155.

Nandi, A., & Shakoor, A. (2009). A GIS-based landslide susceptibility evaluation using bivariate and multivariate statistical analyses. *Engineering Geology, 110*, 11–20.

Ohlmacher, G. C. (2007). Plan curvature and landslide probability in regions dominated by earth flows and earth slides. *Engineering Geology, 91*, 117–134.

Olsen, L. M., Dale, V. H., & Foster, T. (2007). Landscape patterns as indicators of ecological change at Fort Benning, Georgia, USA. *Landscape and Urban Planning, 79*, 137–149.

O'Neill, R. V., Hunsaker, C. T., Jones, K. B., Riitters, K. H., Wickham, J .D., Schwartz, P. M., Goodman, I. A., Jackson, B. L., & Baillargeon, W. S. (1997). Monitoring environmental quality at the landscape scale. *BioScience, 47*, 513–520.

Paudel, S., & Yuan, F. (2012). Assessing landscape changes and dynamics using patch analysis and GIS modeling. *International Journal of Applied Earth Observation and Geoinformation, 16*, 66–76.

Pearce, J., & Ferrier, S. (2000). Evaluating the predictive performance of habitat models developed using logistic regression. *Ecological Modelling,* 133, 225–245.

Rau, R. J., Lee, J. C., Ching, K. E., Lee, Y. H., Byrne, T. B., & Chen, R. Y. (2012). Subduction-continent collision in southwestern Taiwan and the 2010 Jiashian earthquake sequence. *Tectonophysics,* 578, 107-116.

Reddy, C. S., Rao, K. R. M., Pattanaik, C., & Joshi, P. K. (2008). Assessment of large scale deforestation of Nawarangpur district, Orissa, India: a remote sensing based study. *Environmental Monitoring and Assessment, 154*, 325–335.

Rindfuss, R. R., Walsh, S. J., Turner, B. L., Fox, J., & Mishra, V. (2004). Developing a science of land change: challenges and methodological issues. *Proceedings of the National Academy of Science of the United States of America, 101*(39), 13976–13981.

Ruiz, J., & Domon, G. (2009). Analysis of landscape pattern change trajectories within areas of intensive agricultural use: case study in a watershed of southern Que´bec, Canada. *Landscape Ecology, 24*, 419-432.

Tattoni, C., Ciolli, M., & Ferretti, F. (2011). The fate of priority areas for conservation in protected areas: a fine-scale Markov chain approach. *Environmental Management, 47*, 263–278.

Tu, J. Y., Chou, C., & Chu, P. S. (2009). The abrupt shift of typhoon activity in the vicinity of Taiwan and its association with Western North Pacific–East Asian climate change. *Journal of Climate, 22*(13), 3617-3628.

Turner, M. G. (1989). Landscape ecology: the effect of pattern on process. *Annual Review of Ecology and Systematics*, 20, 171–197..

Turner, M. G., Gardner, R. H., & O'Neill, R. V. (2001). *Landscape ecology in theory and practice: pattern and process*. New York: Springer-Verlag.

Verburg, P. H., van Berkel, D. B., van Door, A. M., van Eupen, M., & van den Heiligenberg, H. A. R. M. (2010). Trajectories of land use change in Europe: a model-based exploration of rural futures. *Landscape Ecology, 25*, 217-232.

Wang, D., Gong, J., Chen, L., Zhang, L., Song, Y., & Yue, Y. (2012). Spatio-temporal pattern analysis of land use/cover change trajectories in Xihe watershed. *International Journal of Applied Earth Observation and Geoinformation, 14*, 12–21.

Wang, D., Gong, J., Chen, L., Zhang, L., Song, Y., & Yue, Y. (2013). Comparative analysis of land use/cover change trajectories and their driving forces in two small watersheds in the western Loess Plateau of China. *International Journal of Applied Earth Observation and Geoinformation, 21*, 241–252.

Webster, P. J., Holland, G. J., Curry, J. A., & Chang, H. -R. (2005). Changes in tropical cyclone number, duration, and intensity in a warming environment. *Science, 309*, 1844-1846.

Weng, Q. (2002). Land use change analysis in the Zhujiang Delta of China using satellite remote sensing, GIS and stochastic modeling. *Journal of Environmental Management, 64*, 273–284.

Wu, Q., Li, H. Q., Wang, R. S., Paulussen, J., He, Y., Wang, M., Wang, B. H., & Wang, Z. (2006a). Monitoring and predicting land use change in Beijing using remote sensing and GIS. *Landscape and Urban Planning, 78*, 322–333.

Wu, Y. M., Chen, Y. G., Chang, C. H., Chung, L. H., Teng, T. L., Wu, F. T., & Wu, C. F. (2006b). Seismogenic structure in a tectonic suture zone: With new constraints from 2006 Mw6.1 Taitung earthquake. *Geophysical Research Letters, 33*, L22305.

Wu, Y. M., Chen, Y. G., Shin, T. C., Kuochen, H., Hou, C. S., Hu, J. C., Chang, C. H., Wu, C. F., & Teng, T. L. (2006c). Coseismic versus interseismic ground deformations, fault rupture inversion and segmentation revealed by 2003 *M*w 6.8 Chengkung earthquake in eastern Taiwan. *Geophysical Research Letters, 33*, L02312.

Xiao, H., & Ji, W. (2007). Relating landscape characteristics to non-point source pollution in mine waste-located watersheds using geospatial techniques. *Journal of Environmental Management, 82*, 111-119.

Zhou, Q., Li, B., & Kurban, A. (2008a). Trajectory analysis of land cover change in arid environment of China. *International Journal of Remote Sensing, 29*(4), 1093-1107.

Zhou, Q., Li, B., & Kurban, A. (2008b). Spatial pattern analysis of land cover change trajectories in Tarim Basin, northwest China. *International Journal of Remote Sensing, 29*(19), 5495-5509.

Zonneveld, I. S. (1990). Scope and concepts of landscape ecology as an emerging science. In Zonneveld, I. S., & Forman, R. T. T. (Eds.), *Changing landscapes: an ecological perspective*. New York: Springer-Verlag.

謝　　辭

隨著此文的完稿，四年的研究所求學生涯即將暫告一段落。然而，一本論文的完成，不僅需要個人的努力，背後亦緊密牽動著眾人的投入與付出，此刻心中所湧現的是對這些默默付出的人的無限感恩。

本論文得以順利付梓，首先必須感謝恩師 廖學誠教授。承蒙老師於研究概念之啓迪，本論文得以開展。論文撰寫期間，老師亦不時指引學生方向，每每於研究架構及內容上悉心指導，引領學生於研究之路上持續前進。與老師相識至今已十年有餘，老師於待人接物方面之諸多提點及人生目標之指引，讓學生受益良多，內心感恩之情，不可言喻。

論文初稿，蒙政治大學地政學系詹進發副教授、臺北教育大學社會與區域發展學系蔡元芳教授、臺灣大學地理環境資源學系黃誌川助理教授、本系沈淑敏副教授及郭乃文教授等諸位老師用心審閱，匡正謬誤，以及口試時老師們惠賜卓見，使本文更臻於完善，學生由衷感謝。

感謝林業試驗所中埔研究中心黃正良主任於第一次論文發表中，提供寶貴意見。論文第二次發表中，感謝張瑞津老師以地形學專業角度提供精闢見解；感謝歐陽鍾玲主任提供未來研究方向之建議；感謝沈淑敏老師對研究方法及內容提供深入而透澈的分析，老師的卓見使我深知自己應再持續努力。

研究期間，感謝政治大學詹進發老師於衛星影像判釋技術上的指導；感謝逢甲大學莊永忠老師及學長於遙測技術上的指導；感謝本系洪政耀學長於 GIS 技術上的指點。修課期間，感謝郭乃文老師於研究觀點及方法上的教導；懷念同窗好友，伯鋒、雅韻、燕儀彼此間的相互學習與勉勵；亦感謝坪林國中諸位同仁的支持與關懷。

感謝父母及家人的支持與鼓勵，你們的平安快樂讓我無後顧之憂地完成學業。感謝妻子懿凡一直以來的體諒與包容，妳爲家庭付出的辛勞，讓我能在學術研究

上灌注大部分心力，妳的支持，更是我繼續前進的動力。

如果沒有你們的幫助與鼓勵，此文必將無法順利完稿，僅以此文獻上我對你們無限的感激與祝福，謝謝你們，也將此獻給我即將出生的小寶。

葉春國　謹誌於　師大地理系

2014 年．夏